Journal of Health, Medicine and Nursing www.iiste.org

An Open Access Journal, Vol. 6, 2014

Phenomenon of Biological Adaptation to Heavy Water

Oleg Mosin[1] Ignat Ignatov[2*]

1. PhD (Chemistry), Biotechnology Department, Moscow State University of Applied Biotechnology, Talalikhina Street, 33, Moscow 109316, Russian Federation

2. DSc, Professor, Scientific Research Center of Medical Biophysics (SRCMB), N. Kopernik Street, 32, Sofia 1111, Bulgaria

* E-mail of the corresponding author: mbioph@dir..bg

Abstract

Biological influence of deuterium oxide to cells of various taxonomic groups of prokaryotic and eucaryotic microorganisms realizing methylotrophic, chemoheterotrophic, photo-organotrophic, and photosynthetic ways of assimilation of carbon substrates (methylotrophic bacteria *Brevibacterium methylicum*, chemoheterotrophic bacteria *Bacillus subtilis*, photo-organotrophic halobacteria *Halobacterium halobium*, and single sell green algae *Chlorella vulgaris*) was investigated at the growth on media with ^2H_2O. For investigated microorganisms are submitted the data on growth and adaptation on the growth media containing as sources of deuterated substrates ^2H_2O, [^{2}H]methanol and hydrolisates of deutero-biomass of methylotrophic bacteria *B. methylicum*, obtained after multistage adaptation to ^2H_2O. The qualitative and quantitative composition of intra- and endocellular amino acids, proteins, carbohydrates and fatty acids in conditions of adaptation to ^2H_2O is investigated. It is demonstrated that the effects observed at adaptation to ^2H_2O, possess a complex multifactorial character and connected to cytological, morphological and physiological changes – the magnitude of the lag- period, time of cellular generation, output of biomass, a parity ratio of synthesized amino acids, proteins, carbohydrates and lipids, and also with an evolutionary level of the organization of the investigated object and the pathways of assimilation of carbon substrates as well. These data suggest that adaptation to deuterium oxide is a multifactorial phenomenon, affecting many cellular systems, as biosynthesis of macromolecules, metabolism, transport functions of cells.

Key words: deuterium, deuterium oxide, adaptation, isotopic effects, bacteria, micro algae.

Introduction

The most interesting biological phenomenon is the ability of some microorganisms to grow on heavy water (^2H_2O) media in which all hydrogen atoms are replaced with deuterium (Ignatov & Mosin, 2013a; Ignatov & Mosin, 2013b). ^2H_2O has high environmental potential in biomedical studies due to the absence of radioactivity and poccebility of detecting the deuterium label in the molecule by high-resolution methods as NMR, IR, and mass spectrometry that facilitates its use as a tracer in biochemical and biomedical research (Kushner *et al*., 1999).

The average ratio of $^{1}H/^{2}H$ in nature makes up approximately 1:5700 (Lis *et al*., 2008). In natural waters, the deuterium is distributed irregularly: from 0.02–0.03 mol.% for river water and sea water, to 0.015 mol.% for water of Antarctic ice – the most purified from deuterium natural water containing in 1.5 times less deuterium than that of seawater. According to the international SMOW standard isotopic shifts for ^{2}H and ^{18}O in sea water: $^{2}H/^{1}H = (155.76 \pm 0.05) \cdot 10^{-6}$ (155.76 ppm) and $^{18}O/^{16}O = (2005.20 \pm 0.45) \cdot 10^{-6}$ (2005 ppm). For SLAP standard isotopic shifts for ^{2}H and ^{18}O in seawater make up $^{2}H/^{1}H = 89 \cdot 10^{-6}$ (89 ppm) and for a pair of $^{18}O/^{16}O = 1894 \cdot 10^{-6}$ (1894 ppm). In surface waters, the ratio $^{2}H/^{1}H = \sim(1.32–1.51) \cdot 10^{-4}$, while in the coastal seawater – $\sim(1.55–1.56) \cdot 10^{-4}$. The natural waters of CIS countries are characterized by negative deviations from SMOW standard to $(1.0–1.5) \cdot 10^{-5}$, in some places up to $(6.0–6.7) \cdot 10^{-5}$, but however there are also observed positive deviations at $2.0 \cdot 10^{-5}$.

The chemical structure of $^{2}H_2O$ molecule is analogous to that one for H_2O, with small differences in the length of the covalent H–O-bonds and the angles between them. The molecular mass of $^{2}H_2O$ exceeds on 10% that one for H_2O. The difference in nuclear masses stipulates the isotopic effects, which may be sufficiently essential for the $^{1}H/^{2}H$ pair (Lobishev & Kalinichenko, 1978). As a result, physical-chemical properties of $^{2}H_2O$ differ from H_2O: $^{2}H_2O$ boils at 101.44 ^{0}C, freezes at 3.82 ^{0}C, has maximal density at 11.2 ^{0}C (1.106 g/cm^3) (Vertes, 2004). In mixtures of $^{2}H_2O$ with H_2O the isotopic exchange occurs with high speed with the formation of semi-heavy water ($^{1}H^{2}HO$): $^{2}H_2O + H_2O = {}^{1}H^{2}HO$. For this reason deuterium presents in smaller content in aqueous solutions in form of $^{1}H^{2}HO$, while in the higher content – in form of $^{2}H_2O$. The chemical reactions in $^{2}H_2O$ are somehow slower compared to H_2O. $^{2}H_2O$ is less ionized, the dissociation constant of $^{2}H_2O$ is smaller, and the solubility of the organic and inorganic substances in $^{2}H_2O$ is smaller compared to these ones in H_2O (Mosin, 1996a). Due to isotopic effects the hydrogen bonds with the participation of deuterium are slightly stronger than those ones formed of hydrogen.

For a long time it was considered that heavy water was incompatible with life. Experiments with the growing of cells of different organisms in $^{2}H_2O$ show toxic influence of deuterium. The high concentrations of $^{2}H_2O$ lead to the slowing down the cellular metabolism, mitotic inhibition of the prophase and in some cases – somatic mutations (Den'ko, 1970). This is observed even while using natural water with an increased content of $^{2}H_2O$ or $^{1}H^{2}HO$ (Stom *et al*., 2006). Bacteria can endure up to 90 % (v/v) $^{2}H_2O$, plant cells can develop normally in up to 75 % (v/v) $^{2}H_2O$, while animal cells – up to not more than 30 % (v/v) $^{2}H_2O$ (Mosin & Ignatov, 2012a). Further increase in the concentration of $^{2}H_2O$ for these groups of organisms leads to the cellular death (Katz, 1960; Thomson, 1960), although isolated cell's cultures suspended in pure $^{2}H_2O$ exert a strong radioprotective effect in $^{2}H_2O$-solutions towards γ–radiation (Michel *et al*., 1988; Laeng *et al*., 1991). On the contrary, deuterium depleted water with decreased deuterium content has benefitial effects on organism and stimulates the cellular metabolism (Somlyai, 2001; Sinyak *et al*., 2003).

With the development of new microbiological approaches, there appears an opportunity to use adapted to deuterium cells for preparation of deuterated natural compounds (Mosin *et al*., 2013a; Mosin *et al*., 2013b; Mosin *et al*., 2013c). The traditional method for production of deuterium labelled compounds consists in the growth on media containing maximal concentrations of $^{2}H_2O$ and deuterated substrates as [^{2}H]methanol, [^{2}H]glucose etc. (Mosin & Ignatov, 2012b; Mosin *et al*., 2014). During growth of cells on $^{2}H_2O$ are synthesized molecules of biologically important natural compounds (DNA, proteins, amino acids, nucleosides,

carbohydrates, fatty acids), which hydrogen atoms at the carbon backbones are completely substituted with deuterium. They are isolated from deuterated biomass obtained on growth media with high ^2H_2O content and deuterated substrates with using a combination of physico-chemical methods of separation – hydrolysis, precipitation, extraction with organic solvents and chromatographic purification by column chromatography on different adsorbents. These deuterated molecules evidently undergo structural adaptational modifications necessary for the normal functioning in ^2H_2O.

The adaptation to ^2H_2O is interested not only from scientific point, but allows to obtain the unique biological material for the studying of molecular structure by ^{1}H-NMR (Crespi, 1989). Trend towards the use of deuterium as an isotopic label are stipulated by the absence of radioactivity and possebility of determination the deuterium localization in the molecule by high resolution NMR spectroscopy (LeMaster, 1990), IR spectroscopy (MacCarthy, 1985) and mass spectrometry (Mosin *et al*., 1996a). The recent advances in technical and computing capabilities of these analytical methods have allowed to considerable increase the efficiency of *de novo* biological studies, as well as to carry out structural-functional biophysical studies with deuterated molecules on a molecular level.

This study is a continuation of our research into the adaptation to deuterium of various procaryotic and eucaryotic organisms. The purpose of our research was studying the influence of deuterium on the cells of different taxonomic groups of microorganisms and microalgae realizing methylotrophic, chemoheterotrophic, photo-organotrophic and photosynthetic pathways of carbon assimilation.

2. Material and Methods

2.1. Biological Objects

The objects of the study were various microorganisms, realizing methylotrophic, chemoheterotrophic, photo-organotrophic, and photosynthetic ways of assimilation of carbon substrates. The initial strains were obtained from the State Research Institute of Genetics and Selection of Industrial Microorganisms (Moscow, Russia):

1. *Brevibacterium methylicum B-5652*, a leucine auxotroph Gram-positive strain of facultative methylotrophic bacterium, L-phenylalanine producer, assimilating methanol via the NAD^+ dependent methanol dehydrogenase variant of ribulose-5-monophosphate cycle (RuMP) of carbon fixation.
2. *Bacillus subtilis B-3157*, a polyauxotrophic for histidine, tyrosine, adenine, and uracil spore-forming aerobic Gram-positive chemoheterotrophic bacterium, inosine producer, realizing hexose-6-mono-phosphate (GMP) cycle of carbohydrates assimilation.
3. *Halobacterium halobium ET-1001*, photo-organotrophic carotenoid-containing strain of extreme halobacteria, synthesizing the photochrome transmembrane protein bacteriorhodopsin.
4. *Chlorella vulgaris B-8765*, photosynthesizing single-cell blue-green algae.

2.2. Chemicals

For preparation of growth media was used ^2H_2O (99.9 atom.%), ^{2}HCl (95.5 atom.%) and [^{2}H]methanol (97.5 atom% ^{2}H), purchased from the "Isotope" Russian Research Centre (St. Petersburg, Russian Federation).

Inorganic salts and D- and L-glucose ("Reanal", Hungary) were preliminary crystallized in ^2H_2O and dried in vacuum before using. ^2H_2O was distilled over $KMnO_4$ with the subsequent control of isotope enrichment by ^{1}H-NMR-spectroscopy on a Brucker WM-250 device ("Brucker", Germany) (working frequency: 70 MHz, internal standard: Me_4Si). According to ^{1}H-NMR, the level of isotopic purity of growth media usually was by ~8–10 atom% lower than the isotope purity of the initial ^2H_2O.

2.3. Adaptation Technique

The initial microorganisms were modified by adaptation to deuterium by plating individual colonies onto 2% (w/v) agarose growth media with stepwise increasing gradient of ^2H_2O concentration and subsequent selection of individual cell colonies stable to the action of ^2H_2O. As a source of deuterated growth substrates for the growth of chemoheterotrophic bacteria and chemoorganoheterotrophic bacteria was used the deuterated biomass of facultative methylotrophic bacterium *B. methylicum*, obtained via a multi-stage adaptation on solid 2% (w/v) agarose M9 media with an increasing gradient of ^2H_2O (from 0, 24.5, 49.0, 73.5 up to 98% (v/v) ^2H_2O). Raw deuterated biomass (output, 100 gram of wet weight per 1 liter of liquid culture) was suspended in 100 ml of 0.5 N ^{2}HCl (in ^2H_2O) and autoclaved for 30–40 min at 0.8 atm. The suspension was neutralized with 0.2 N KOH (in ^2H_2O) to pH = 7.0 and used as a source of growth substrates while adaptation and growing the chemoheterotrophic bacterium *B. sublilis* and the photo-organotrophic halobacterium *H. halobium*.

2.4. Growth Media

The following growth media were used (concentratioin of components are given in g/l):

1. Minimal salt medium M9 for growth of the facultative methanol assimilating methylotrophic bacterium *B. methylicum B-5662*, supplemented with 2% (v/v) [^{2}H]methanol and increasing gradient of ^2H_2O concentration from 0; 24.5; 49.0; 73.5 up to 98 % (v/v) ^2H_2O: KH_2PO_4 – 3; Na_2HPO_4 – 6; NaCl – 0.5; NH_4Cl – 1; L-leucine – 0.01.

2. Hydrolysated medium HM1 for growth of the aerobic Gram-positive chemoheterotrophic bacterium *B. subtilis B-3157*, based on ^2H_2O (89–90 atom% ^{2}H) and 2% (w/v) hydrolysate of deuterated biomass of *B. methylicum B-5662* as a source of ^{2}H-labeled growth substrates: L-glucose –120; hydrolysate of deuterated biomass of *B. methylicum* – 20, NH_4NO_3 – 20; $MgSO_4 \cdot 7H_2O$ – 10; $CaCO_3$ – 20; adenine, and uracil – 0.01. As a control was used protonated medium containing 2% (w/v) yeast protein–vitamin concentrate (PVC).

3. Hydrolysated medium HM2 for the growth of the extreme aerobic halobacterium *Halobacterium halobium ET-1001* (based on 99.9 atom% ^2H_2O): NaCl - 250; $MgSO_4 \cdot 7H_2O$ - 20; KCl - 2; $CaCl_2 \cdot 6H_2O$ – 0.065; sodium citrate - 0.5; hydrolyzate of deuterated biomass of *B. methylicum B-5662* – 20; biotin – $1 \cdot 10^{-4}$; folic acid – $1.5 \cdot 10^{-4}$, vitamin B_{12} – $2 \cdot 10^{-5}$).

4. Tamiya medium for the growth of the photosynthetic green microalgae *C. vulgaris B-8765* (based on 99.9 atom% ^2H_2O): KNO_3 – 5.0; $MgSO_4 \cdot 7H_2O$ – 2.5; KH_2PO_4 – 1.25; $FeSO_4$ – 0.003; $MnSO_4 \cdot 2H_2O$ – $3 \cdot 10^{-4}$; $CaCl_2 \cdot 6H_2O$ – 0.065; $ZnSO_4 \cdot 7H_2O$ – $4 \cdot 10^{-5}$; $CuSO_4 \cdot 5H_2O$ – $5 \cdot 10^{-5}$, $CoCl_2 \cdot 6H_2O$ – $5 \cdot 10^{-6}$).

2.5. Growth Conditions

The cells were grown in 500 ml Erlenmeyer flasks containing 100 ml of the growth medium at 32–34 ^{0}C and

vigorously aerated on an orbital shaker Biorad ("Biorad Labs", Poland). Photo-organotrophic bacteria and blue-green algae were grown at illumination by fluorescent monochromatic lamps LDS-40-2 (40 W) ("Alfa-Electro", Russia). Growing of microalgae *C. vulgaris* was carried out at 32 ^{0}C in a photoreactor with CO_2 bubbling. The bacterial growth was monitored on the ability to form individual colonies on the surface of solid 2 % (w/v) agarose media, as well as on the optical density of the cell suspension measured on a Beckman DU-6 spectrophotometer ("Beckman Coulter", USA) at λ = 620 nm. After 6–7 days the cells were harvested and separated by centrifugation (10000 g, 20 min) on T-24 centrifuge ("Heracules", Germany). The biomass was washed with ^2H_2O and extracted with a mixure of organic solvents: chloroform–methanol–acetone = 2:1:1, % (v/v) for isolating lipids and pigments. The resulting precipitate (10−12 mg) was dried in vacuum and used as a protein fraction, while the liquid extract – as a lipid fraction. The exogenious deuterated amino acids and ribonucleosides were isolated from culture liquids (CL) of appropriate strain-producers. Inosine was isolated from the CL of *B. subtilis* by adsorption/desorption on activated carbon as adsorbent with following extraction with 0.3 M NH_4-formate buffer (pH = 8.9), subsequent crystallization in 80 % (v/v) ethanol, and ion exchange chromatography (IEC) on a column with cation exchange resin AG50WX 4 equilibrated with 0.3 M NH_4-formate buffer and 0.045 M NH_4Cl (output, 3.1 g/l (80 %); $[\alpha]_D^{20}$ = 1.61 (ethanol)). Bacteriorhodopsin was isolated from the purple membranes of photo-organotrophic halobacterium *H. halobium* by the method of D. Osterhelt, modificated by the authors, with using SDS as a detergent (Mosin *et al*., 1999a).

2.6. Protein Hydrolysis

Dry biomass (10 g) was treated with a chloroform–methanol–acetone mixture (2:1:1, % (v/v)) and supplemented with 5 ml of 6 N ^2HCl (in ^2H_2O). The ampules were kept at 110 ^{0}C for ~24 h. Then the reaction mixture was suspended in hot ^2H_2O and filtered. The hydrolysate was evaporated at 10 mm Hg. Residual ^2HCl was removed in an exsiccator over solid NaOH.

2.7. Hydrolysis of Intracellular Policarbohydrates

Dry biomass (50 mg) was placed into a 250 ml round bottomed flask, supplemented with 50 ml distilled ^2H_2O and 1.6 ml of 25% (v/v) H_2SO_4 (in ^2H_2O), and boiled in a reflux water evaporator for ~90 min. After cooling, the reaction mixture was suspended in one volume of hot distilled ^2H_2O and neutralized with 1 N $Ba(OH)_2$ (in ^2H_2O) to pH = 7.0. $BaSO_4$ was separated by centrifugation (1500 g, 5 min); the supernatant was decanted and evaporated at 10 mm Hg.

2.8. Amino Acid Analysis

The amino acids of the hydrolyzed biomass were analyzed on a Biotronic LC-5001 (230×3.2) column ("Eppendorf–Nethleler–Hinz", Germany) with a UR-30 sulfonated styrene resin ("Beckman–Spinco", USA) as a stationary phase; the temperature – 20±25 ^{0}C; the mobile phase – 0.2 N sodium–citrate buffer (pH = 2.5); the granule diameter – 25 μm; working pressure – 50–60 atm; the eluent input rate – 18.5 ml/h; the ninhydrin input rate – 9.25 ml/h; detection at λ = 570 and λ = 440 nm (for proline).

2.9. Analysis of Carbohydrates

Carbohydrates were analyzed on a Knauer Smartline chromatograph ("Knauer", Germany) equipped with a Gilson pump ("Gilson Inc.", USA) and a Waters K 401 refractometer ("Water Associates", USA) using Ultrasorb CN column (250×10 mm) as a stationary phase; the temperature – 20±25 ^{0}C; the mobile phase – acetonitrile–water (75:25, % (w/w); the granule diameter – 10 μm; the input rate – 0.6 ml/min.

2.10. Analysis of Fatty Acids

Fatty acids were analyzed on a Beckman Gold System (USA) chromatograph (250×4.6 mm), equiped with Model 126 UV-Detector (USA), 20±25 ^{0}C . Stationary phase – Ultrasphere ODS 5 μm; mobile phase – linear gradient of 5 mM KH_2PO_4–acetonitrile; elution rate – 0.5 ml/min, detection at λ = 210 nm.

2.11. Mass Spectrometry

For evaluation of deuterium enrichment levels EI and FAB mass spectrometry was used. EI mass spectra were recorded on MB-80A device ("Hitachi", Japan) with double focusing (the energy of ionizing electrons – 70 eV; the accelerating voltage – 8 kV; the cathode temperature – 180–200 ^{0}C) after amino acid modification into methyl esters of N-5-dimethylamino(naphthalene)-1-sulfonyl (dansyl) amino acid derivatives according to an earlier elaborated protocol (Mosin *et al*., 1998). FAB-mass spectra were recorded on a VG-70 SEQ chromatograph ("Fisons VG Analytical", USA) equipped with a cesium Cs^+ source on a glycerol matrix with accelerating voltage 5 kV and ion current 0.6–0.8 mA. Calculation of deuterium enrichment of the molecules was carried out using the ratio of contributions of molecular ion peaks of deuterated compounds extracted on D_2O-media relative to the control obtained on H_2O.

2.6. Scanning Electrom Microscopy (SEM)

SEM was carried out on JSM 35 CF (JEOL Ltd., Korea) device, equiped with SE detector, thermomolecular pump, and tungsten electron gun (Harpin type W filament, DC heating); working pressure – 10^{-4} Pa (10^{-6} Torr); magnification – ×150.000, resolution – 3.0 nm, accelerating voltage – 1–30 kV; sample size – 60–130 mm.

2.12. IR-spectroscopy

IR-spectroscopy was performed on Brucker Vertex spectrometer ("Brucker", Germany) (spectral range: average IR – 370–7800 cm^{-1}; visible – 2500–8000 cm^{-1}; the permission – 0.5 cm^{-1}; accuracy of wave number – 0.1 cm^{-1} on 2000 cm^{-1}).

3. Results

3.1. Adaptation to deuterium the methylotrophic bacterium B. methylicum

Numerous studies carried out by us with various biological objects in ^2H_2O, proved that when biological objects being exposed to water with different deuterium content, their reaction varies depending on the isotopic composition of water (the content of deuterium in water) and magnitude of isotope effects determined by the difference of constants of chemical reactions rates k_H/k_D in H_2O and ^2H_2O. The maximum kinetic isotopic effect

observed at ordinary temperatures in chemical reactions leading to rupture of bonds involving hydrogen and deuterium atoms lies in the range k_H/k_D = 5–8 for C–H versus C–^{2}H, N–^{2}H versus N–^{2}H, and O–^{2}H versus O–^{2}H-bonds (Mosin, 1996; Mosin & Ignatov, 2012a; Mosin & Ignatov, 2012b). Isotopic effects have an impact not only on the physical and chemical properties of deuterated macromolecules in which H atoms are substituted with ^{2}H atoms, but also on the biological behaviour of biological objects in ^2H_2O. Experiments with ^2H_2O (Table 1) have shown, that green-blue algae is capable to grow on 70 % (v/v) ^2H_2O, methylotrophic bacteria – 75 % (v/v) ^2H_2O, chemoheterotrophic bacteria – 82 % (v/v) ^2H_2O, and photo-organotrophic halobacteria – 95 % (v/v) ^2H_2O.

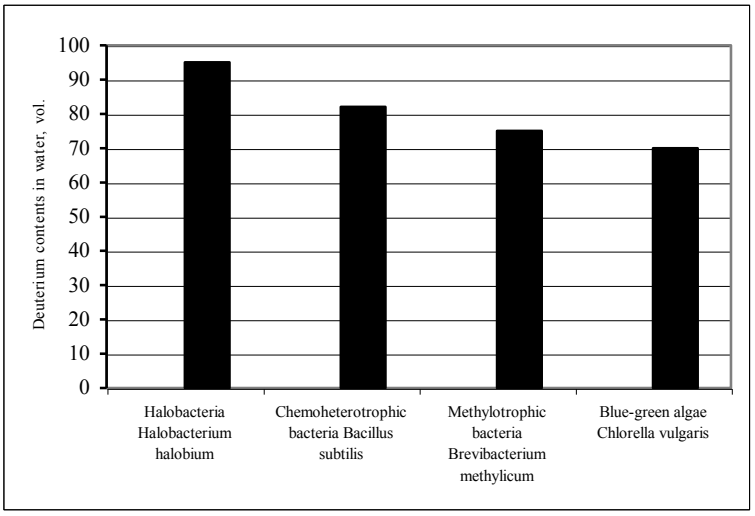

Figure 1. Cell survival of various microorganisms in water with different deuterium content (%, v/v)

In the course of the experiment were obtained adapted to the maximum concentration of ^2H_2O cells belonging to different taxonomic groups of microorganisms, realizing methylotrophic, chemoheterotrophic, photo-organotrophic and photosynthetic pathways of assimilation of carbon substrata, as facultative methylotrophic bacterium *B. methylicum*, chemoheterotrophic bacterium *B. subtilis*, halobacterium *H. halobium* and blue-green algae *C. vulgaris*.

Selection of methanol-assimilating facultative methylotrophic bacterium *B. methylicum* was connected with the development of new microbiological strategies for preparation of deuterated biomass via bioconversion of [^{2}H]methanol and ^2H_2O and its further use as a source of deuterated growth substrates for the growing other strains-producers in ^2H_2O.

Choosing of photo photo-organotrophic halobacterium *H. halobium* was stipulated by the prospects of further isolation of retinal containing transmembrane protein bacteriorhodopsin (BR) – chromoprotein of 248 amino acid residues, containing as a chromophore an equimolar mixture of 13-*cis*-and 13-*trans* C20 carotenoid associated with a protein part of the molecule via a Lys-216 residue (Mosin & Ignatov, 2014). BR performs in the cells of halobacteria the role of ATP-dependent translocase, which creates an electrochemical gradient of H^+ on the surface of the cell membrane, which energy is used by the cell for the

synthesis of ATP in the anaerobic photosynthetic phosphorylation.

Using chemoheterotrophic bacterium *B. subtilis* was determined by preparative isolation produced by this bacterium deuterated ribonucleoside – inosine (total deuteration level 65.5 atom.% ^2H) for biomedical use (Mosin & Ignatov, 2013d), and the use of photosynthetic blue-green *C. vulgaris* was stipulated by the study of biosynthesis of deuterated chlorophyll and carotenoid pigments (deuteration level 95–97 atom.% ^2H) on growth media with high ^2H_2O-content (Mosin & Ignatov, 2012b).

We used stepwise increasing gradient concentration of ^2H_2O in growth media, because it was assumed that the gradual accustoming of micorganisms to deuterium would have a beneficial effect upon the growth and physiological parameters. The strategy of adaptation to ^2H_2O is shown in Table. 1 on an example of methylotrophic bacterium *B. methylicum*, which deuterated biomass was used in further experiments as a source of deuterated growth substrates for growing of chemoheterotrophic and photo-organotrophic bacteria. For this, deuterium enrichment technique was applied *via* plating cell colonies on 2% (w/v) agarose M9 media supplemented with 2% (v/v) [U-^2H]MeOH with an increase in the ^2H_2O content from 0; 24.5; 49.0; 73.5 up to 98% (v/v) ^2H_2O, combined with subsequent selection of cell colonies which were resistant to deuterium. The degree of cell survive on maximum deuterated medium was approx. 40%. The data on the yield of biomass of initial and adapted *B. methylicum*, magnitude of lag-period and generation time on protonated and maximum deuterated M9 medium are shown in Figure 2. The yield of biomass for adapted methylotroph (*c*) was decreased approx. on 13% in comparison with control conditions (*a*) at an increase in the time of generation up to 2.8 h and the lag-period up to 40 h (Figure 1). As is shown from these data, as compared with the adapted strain, the growth characteristics of initial strain on maximally deuterated medium were inhibited by deuterium.

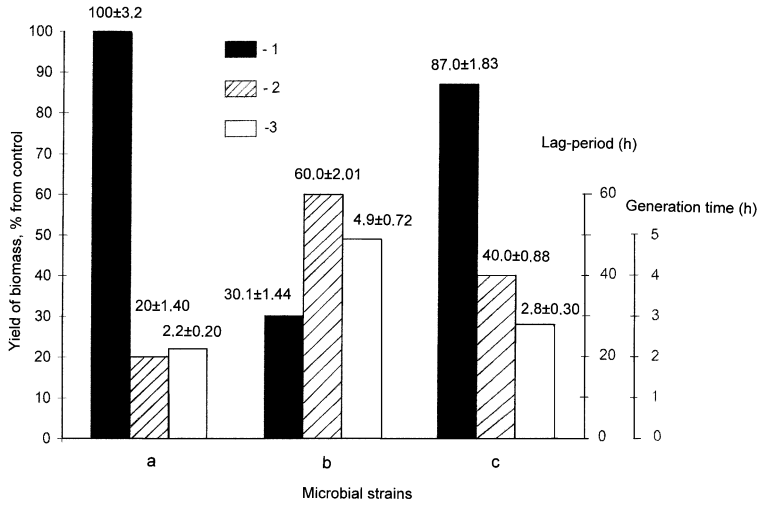

Figure 2. Yield of microbial biomass of *B. methylicum*, magnitude of lag-period and generation time in various experimental conditions: initial strain on protonated M9 medium (control) with water and methanol (*a*); initial strain on maximally deuterated M9 medium (b); adapted to deuterium strain on maximally

deuterated M9 medium (c): 1 – yield of biomass, % from the control; 2 – duration of lag-period, h; 3 – generation time, h.

Experimental conditions are given in Table 1 (expts. 1–10) relative to the control (expt. 1) on protonated medium M9 and to the adapted bacterium (expt. 10'). Various compositions of [U-^{2}H]MeOH and ^2H_2O were added to growth media M9 as hydrogen/deuterium atoms could be assimilated both from MeOH and H_2O. The maximum deuterium content was under conditions (10) and (10') in which we used 98% (v/v) ^2H_2O and 2% (v/v) [U-^{2}H]MeOH. The even numbers of experiment (Table 1, expts. 2, 4, 6, 8, 10) were chosen to investigate whether the replacement of MeOH by its deuterated analogue affected growth characteristics in presence of ^2H_2O. That caused small alterations in growth characteristics (Table 1, expts. 2, 4, 6, 8, 10) relative to experiments, where we used protonated methanol (Table 1, expts. 3, 5, 7, 9). The gradual increment in the concentration of ^2H_2O into growth medium caused the proportional increase in lag-period and yields of microbial biomass in all isotopic experiments. Thus, in the control (Table 1, expt. 1), the duration of lag-period did not exceed 20.2 h, the yield of microbial biomass (wet weight) and production of phenylalanine were 200.2 and 0.95 gram per 1 liter of growth medium. The adding gradually increasing concentrations of ^2H_2O into growth media caused the proportional increasing of *lag*-period and yield of microbial biomass in all isotopic experiments. The results suggested, that below 49% (v/v) ^2H_2O (Table 1, expts. 2–4) there was a small inhibition of bacterial growth compared with the control (Table 1, expt. 1). However, above 49% (v/v) ^2H_2O (Table 1, expts. 5–8), growth was markedly reduced, while at the upper content of ^2H_2O (Table 1, expts. 9–10) growth got 3.3-fold reduced. With increasing content of ^2H_2O in growth media there was a simultaneous increase both of lag-period and generation time. Thus, on maximally deuterated growth medium (Table 1, expt. 10) with 98% (v/v) ^2H_2O and 2% (v/v) [U-^{2}H]MeOH, lag-period was 3 fold higher with an increased generation time to 2.2 fold as compared to protonated growth medium with protonated water and methanol which serve as control (Table 1, expt. 1). While on comparing adapted bacterium on maximally deuterated growth medium (Table 1, expt. 10') containing 98% (v/v) ^2H_2O and 2% (v/v) [U-^{2}H]MeOH with non adapted bacterium at similar concentration showed 2.10 and 2.89 fold increase in terms of phenylalanine production and biomass yield due to deuterium enrichment technique, while, the lag phase as well as generation time also got reduced to 1.5 fold and 1.75 fold in case of adapted bacterium.

The adapted bacterium of *B. methylicum* eventually came back to normal growth at placing over in protonated growth medium after some lag-period that proves phenotypical nature of a phenomenon of adaptation that was observed for others adapted by us strains of methylotrophic bacteria and representatives of other taxonomic groups of microorganisms [Mosin & Ignatov, 2012a; Mosin & Ignatov, 2013a, Ignatov & Mosin, 2013b]. Literature reports clearly reveal that the transfer of deuterated cells to protonated medium M9 eventually after some lag period results in normal growth that could be due to the phenomenon of adaptation wherein phenotypic variation was observed by the strain of methylotrophic bacteria (Mosin & Ignatov, 2013b; Mosin et al., 2013). The improved growth characteristics of adapted methylotroph essentially simplify the scheme of obtaining the deutero-biomass which optimum conditions are M9 growth medium with 98% ^2H_2O and 2% [^{2}H]methanol with incubation period 3–4 days at temperature 35 ^{0}C.

Table 1. Effect of variation in isotopic content (0–98% ^2H_2O, v/v) in growth media M9 on bacterial growth of *B. methylicum* and phenylalanine production

Bacterial strains	Exp. number	Media components, % (v/v)				Lag-period (h)	Yield in terms of wet biomass (g/l)	Generation time (h)	Phenylalanine production (g/l)
		H_2O	^2H_2O	MeOH	[U-^{2}H] MeOH				
Non adapted	1(control)	98.0	0	2	0	20.2 ±1.40	200.2 ±3.20	2.2 ±0.2	0.95 ±0.12
Non adapted	2	98.0	0	0	2	20.3 ±1.44	184.6 ±2.78	2.4 ±0.2	0.92 ±0.10
Non adapted	3	73.5	24.5	2	0	20.5 ±0.91	181.2 ±1.89	2.4 ±0.2	0.90 ±0.10
Non adapted	4	73.5	24.5	0	2	34.6 ±0.89	171.8 ±1.81	2.6 ±0.2	0.90 ±0.08
Non adapted	5	49.0	49.0	2	0	40.1 ±0.90	140.2 ±1.96	3.0 ±0.3	0.86 ±0.10
Non adapted	6	49.0	49.0	0	2	44.2 ±1.38	121.0 ±1.83	3.2 ±0.3	0.81 ±0.09
Non adapted	7	24.5	73.5	2	0	45.4 ±1.41	112.8 ±1.19	3.5 ±0.2	0.69 ±0.08
Non adapted	8	24.5	73.5	0	2	49.3 ±0.91	94.4 ±1.74	3.8 ±0.2	0.67 ±0.08
Non adapted	9	98.0	0	2	0	58.5 ±1.94	65.8 ±1.13	4.4 ±0.7	0.37 ±0.06
Non adapted	10	98.0	0	0	2	60.1 ±2.01	60.2 ±1.44	4.9 ±0.7	0.39 ±0.05
Adapted	10’	98.0	0	0	2	40.2 ±0.88	174.0 ±1.83	2.8 ±0.3	0.82 ±0.08

Notes:

* The date in expts. 1–10 described the growth characteristics for non-adapted bacteria in growth media, containing 2 % (v/v) MeOH/[U-^{2}H]MeOH and specified amounts (%, v/v) ^2H_2O.

** The date in expt. 10’ described the growth characteristics for bacteria adapted to maximum content of deuterium in growth medium.

***As the control used exprt. 1 where used ordinary protonated water and methanol

Adaptation, which conditions are shown in experiment 10' (Table 1) was observed by investigation of growth dynamics (expts. 1*a*, 1*b*, 1*c*) and accumulation of L-phenylalanine into growth media (expts. 2*a*, 2*b*, 2*c*) by initial (*a*) and adapted to deuterium (*c*) strain *B. methylicum* in maximum deuterated growth medium M9 (Figure 3, the control (*b*) is obtained on protonated growth medium M9). In the present study, the production of phenylalanine (Figure 2, expts. 1b, 2b, 3b) was studied and was found to show a close linear extrapolation with respect to the time up to exponential growth dynamics (Figure 3, expts. 1a, 2a, 3a). The level of phenylalanine production for non-adapted bacterium on maximally deuterated medium M9 was 0.39 g/liter after 80 hours of growth (Figure 2, expt. 2b). The level of phenylalanine production by adapted bacterium under those growth conditions was 0.82 g/liter (Figure 3, expt. 3b). Unlike to the adapted strain the growth of initial strain and production of phenylalanine in maximum deuterated growth medium were inhibited. The important feature of adapted to ^2H_2O strain *B. methylicum* was that it has kept its ability to synthesize and exogenously produce L-phenylalanine into growth medium. Thus, the use of the adapted bacterium enabled to improve the level of phenylalanine production on maximally deuterated medium by 2.1 times with the reduction in the lag phase up to 20 h. This is an essential achievement for this strain of methylotrophic bacteria, because up till today there have not been any reports about production of phenylalanine by leucine auxotrophic methylotrophs with the NAD^+ dependent methanol dehydrogenase (EC 1.6.99.3) variant of the RuMP cycle of carbon assimilation. This makes this isolated strain unique for production of deuterated phenylalanine and other metabolically related amino acids.

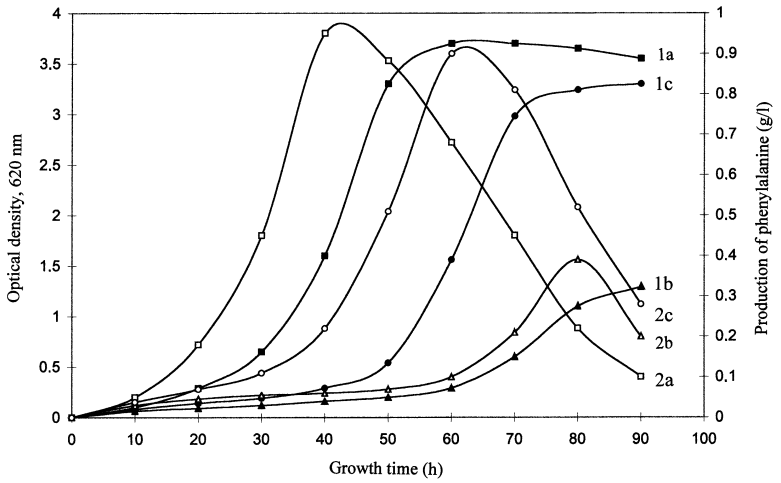

Figure 3. Growth dynamics of *B. methylicum* (1a, 2a, 3a) and production of phenylalanine (1b, 2b, 3b) on media M9 with various isotopic content: 1a, 1b – non-adapted bacterium on protonated medium (Table 1, expt. 1); 2a, 2b – non-adapted bacterium on maximally deuterated medium (Table 1, expt. 10); 3a, 3b – adapted bacterium on maximally deuterated medium (Table 1, expt. 10')

The general feature of phenylalanine biosynthesis in $H_2O/^2H_2O$-media was increase of its production at early exponential phase of growth when outputs of a microbial biomass were insignificant (Figure 3). In all

the experiments it was observed that there was a decrease in phenylalanine accumulation in growth media at the late exponential phase of growth. Microscopic research of growing population of microorganisms showed that the character of phenylalanine accumulation in growth media did not correlate with morphological changes at various stages of the cellular growth. Most likely that phenylalanine, accumulated in growth media, inhibited enzymes of its biosynthetic pathways, or it later may be transformed into intermediate compounds of its biosynthesis, e.g. phenylpyruvate (Maksimova et al., 1990; Skladnev et al., 1996). It is necessary to notice, that phenylalanine is synthesised in cells of microorganisms from prephenic acid, which through a formation stage of phenylpiruvate turns into phenylalanine under the influence of cellular transaminases. However, phenylalanine was not the only product of biosynthesis; other metabolically related amino acids (alanine, valine, and leucine/isoleucine) were also produced and accumulated into growth media in amounts of 5–6 μmol in addition to phenylalanine. This fact required isolation of [^{2}H]phenylalanine from growth medium, which was carried out by extraction of lyophilized LC with iso-PrOH and the subsequent crystallization in EtOH. Analytical separation of [^{2}H]phenylalanine and metabolically related [^{2}H]amino acids was performed using a reversed-phase HPLC method on Separon SGX C_{18} Column, developed for methyl esters of N-DNS-[^{2}H]amino acids with chromatographic purity of 96–98% and yield of 67–89%.

Table 2. Effect of deuterium enrichment levels (atom.%) in the molecules of [^{2}H]amino acids excreted by *B. methylicum**

[^{2}H]amino acid	Concentration of ^2H_2O in growth media, % (v/v)**			
	24.5	49.0	73.5	98.0
Alanine	24.0 ±0.70	50.0 ±0.89	50.0 ±0.83	50.0 ±1.13
Valine	20.0 ±0.72	50.0 ±0.88	50.0 ±0.72	62.5 ±1.40
Leucine/isoleucine	20.0 ±0.90	50.0 ±1.38	50.0 ±1.37	50.0 ±1.25
Phenylalanine	17.0 ±1.13	27.5 ±0.88	50.0 ±1.12	75.0 ±1.40

Notes:

* At calculation of enrichment levels protons (deuterons) at COOH- and NH_2-groups of amino acids were not considered because of dissociation in H_2O (^2H_2O).

** The data on enrichment levels described bacteria grown on minimal growth media M9 containing 2% (v/v) [U-^{2}H]MeOH and specified amounts (%, v/v) ^2H_2O.

With increasing ^2H_2O content in growth media, the levels of deuterium enrichment in exogenous [^{2}H]amino acids (phenylalanine, alanine, valine, and leucine/isoleucine), secreted by *B. methylicum*, were varied proportionally. The similar result on proportional specific increase of levels of deuterium enrichment into [^{2}H]phenylalanine and other metabolically related [^{2}H]amino acids was observed in all isotopic experiments where used increasing concentration ^2H_2O in growth media (Table 2). Predictably, enrichment levels of [^{2}H]phenylalanine related to the family of aromatic amino acids synthesised from shikimic acid and metabolically related [^{2}H]amino acids of pyruvic acid family – alanine, valine and leucine at identical

^2H_2O concentration in growth media are correlated among themselves. Such result is fixed in all isotope experiments with ^2H_2O (Table 2). Unlike [^{2}H]phenylalanine, deuterium enrichment levels in accompanying [^{2}H]amino acids – Ala, Val and Leu/Ile keep a stable constancy within a wide interval of ^2H_2O concentration: from 49% (v/v) to 98% (v/v) ^2H_2O (Table 2). Summarizing these data, it is possible to draw a conclusion on preservation of minor pathways of the metabolism connected with biosynthesis of leucine and metabolic related amino acids of pyruvic acid family – alanine and valine, which enrichment levels were in correlation within identical concentration of H_2O in growth media (phenylalanine is related to the family of aromatic amino acids synthesized from shikimic acid). Since leucine was added into growth media in protonated form, another explanation of this effect, taking into consideration the various biosynthetic pathways of Leu and Ileu (Ileu belongs to the family of aspartic acid, while Leu belongs to the pyruvic acid family), could be cell assimilation of protonated leucine from growth media. Since Leu and Ileu could not be clearly estimated by EI MS method, nothing could be said about possible biosynthesis of [^{2}H]isoleucine. Evidently, higher levels of deuterium enrichment can be achieved by replacement of protonated leucine on its deuterated analogue, which may be isolated from hydrolysates of deuterated biomass of this methylotrophic bacterium.

It should be noted that the yields of biomass on deuterated growth media were varried 85-90% for different taxonomic groups of microorganisms. All adapted microorganisms had a slightly reduced levels of microbial biomass accumulation and increased cell generation times on maximal deuterated media.

3.2. Adaptation to deuterium the chemoheterotrophic bacterium B. subtillis

The result obtained in experiments on the adaptation of methylotrophic bacterium *B. methylicum* to ^2H_2O allowed to use hydrolysates of biomass of this bacterium obtained in the process of multi-stage adaptation to ^2H_2O, as a source of deuterated growth substrates for the growing of the chemoheterotrophic bacterium *B. subtillis* and the photoorganotrophic halobacterium *H. halobium*.

The assimilation rate of methylotrophic biomass by protozoa and eukaryotic cells amounts to 85–98%, while the productivity calculated on the level of methanol bioconversion into cell components makes up 50–60% (Mosin et al., 1999a; Mosin et al., 1999b). While developing the composition of growth media on the basis of deutereted biomass of methylotrophic bacteria *B. methylicum* it was taken into account the ability of methylotrophic bacteria to synthesize large amounts of protein (output, 50% (w/w) of dry weight), 15–17% (w/w) of polysaccharides, 10–12% (w/w) of lipids (mainly, phospholipids), and 18% (w/w) of ash (Mosin & Ignatov, 2013b). To provide high outputs of these compounds and minimize the isotopic exchange (^{1}H–^{2}H) in amino acid residues of protein molecules, the biomass was hydrolyzed by autoclaving in 0.5 N ^{2}HCl (in ^2H_2O) and used for the growing of chemoheterotrophic bacterium B. subtillis and photoorganoheterotrophic halobacteria *H. halobium*.

The methylotrophic hydrolysate, obtained on the maximally deuterated medium M9 with 98% (v/v) ^2H_2O and 2% (v/v) [^{2}H]methanol, contains 15 identified amino acids (except for proline detected at λ = 440 nm) with tyrosine and histidine content per 1 gram of dry methylotrophic hydrolysate 1.82% and 3.72% (w/w), thereby satisfying the auxotrophic requirements of the inosine producer strain for these amino acids (Table 3). The content of other amino acids in the hydrolysate is also comparable with the needs of the strain in

sources of carbon and amine nitrogen. The indicator determining the high efficiency of deuterium incorporation into the synthesized product is high levels of deuterium enrichment of amino acid molecules, varied from 50 atom% ^2H for leucine/isoleucine to 98.5 atom% ^2H for alanine (Table 3).

Table 3. Amino acid composition of hydrolyzed biomass of the facultative methylotrophic bacterium *B. methylicum* obtained on maximally deuterated M9 medium with 98% (v/v) ^2H_2O and 2% (v/v) [^2H]methanol and levels of deuterium enrichment*

Amino acid	Yield, % (w/w) dry weight per 1 gram of biomass	Number of deuterium atoms incorporated into the carbon backbone of a molecule**	Level of deuterium enrichment of molecules, % of the total number of hydrogen atoms***
Glycine	9.55	2	92.5 ±1.86
Alanine	13.30	4	98.5 ±1.96
Valine	4.21	4	52.2 ±1.60
Leucine	8.52	5	50.0 ±1.52
Isoleucine	4.01	5	50.0 ±1.55
Phenylalanine	3.89	8	96.0 ±1.85
Tyrosine	2.10	7	95.5 ±1.82
Serine	3.60	3	86.7 ±1.55
Threonine	4.89	–	–
Methionine	2.62	–	–
Asparagine	10.02	2	68.5 ±1.62
Glutamic acid	10.31	4	70.0 ±1.65
Lysine	3.53	5	59.0 ±1.60
Arginine	4.65	–	–
Histidine	3.98	–	–

Keys: * The data were obtained for methyl esters of N-5-dimethylamino(naphthalene)-1-sulfonyl (dansyl) chloride amino acid derivatives.

** At calculation the level of deuterium enrichment, the protons (deuterons) at COOH- and NH_2- groups of amino acid molecules were not taken into account because of the dissociation in $H_2O/^2H_2O$.

*** A dash denotes the absence of data.

Taking into account the pathways of assimilation of carbon substrates, the adaptation of chemoheterotrophic bacterium *B. subtilis* was carried out via plating of initial cells to separate colonies on solid 2% (w/v) agarose HM1 media based on 99,9 atom% ^2H_2O and deuterated hydrolyzate biomass of B. methylicum, with the following subsequent selection of the colonies resistant to ^2H_2O. On contrary to ^2H_2O,

^{2}H-substrates in composition of deuterated biomass hydrolyzate had no significant negative effect on the growth parameters of the studied microorganisms. The growth and biosynthetic characteristics of inosine-producing strain *B. subtilis* were studied on protonated yeast PVC medium with H_2O and 2% (w/v) yeast PVC and on HW medium with 89% (v/v) ^2H_2O and 2% (w/w) hydrolysate of deuterated biomass of *B. methylicum* (Figure 4). Experiments demonstrated a certain correlation between the changes of growth dynamics of *B. subtilis* (Figure 4, curves *1*, *1*'), output of inosine (Figure 4, curves *2*, *2*'), and glucose assimilation (Figure 4, curves *3*, *3*'). The maximal output of inosine (17 g/l) was observed on protonated PVC medium at a glucose assimilation rate 10 g/l (Figure 4, curve *2*). The output of inosine in the HW medium decreased in 4.4-fold, reaching 3.9 g/l (Figure 4, curve *2*'), and the level of glucose assimilation – 4-fold, as testified by the remaining 40 g/l non-assimilated glucose in CL (Figure 4, curve *3*'). The experimental data demonstrate that glucose is less efficiently assimilated during growth in the HW medium as compared to the control conditions in H_2O.

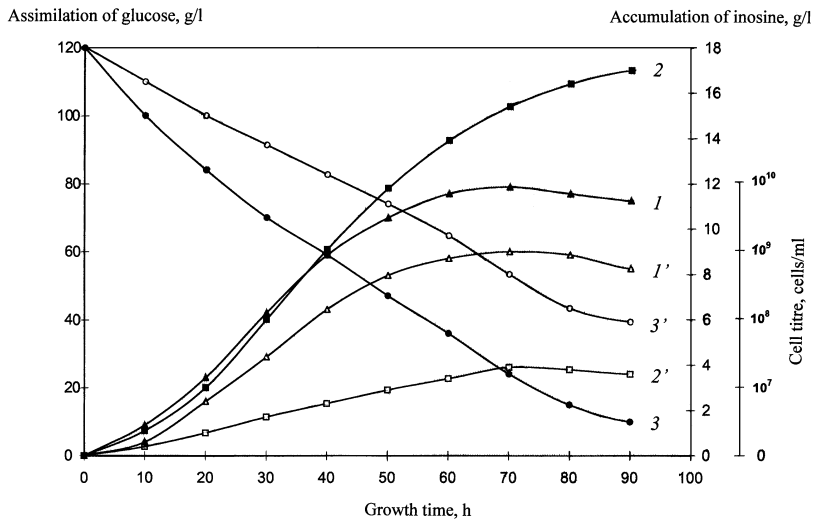

Figure 4. Growth dynamics of *B. subtilis* (*1*, *1*') (cells/ml), inosine accumulation in LC (*2*, *2*') (g/l), and glucose assimilation (*3*, *3*') (g/l) under different experimental conditions: (*1*–*3*) – protonated yeast PVC medium; (*1*'–*3*') – HW medium with 2% (w/v) hydrolysate of deuterated biomass of *B. methylicum*.

The isolation of inosine from the CL consisted in low-temperature precipitation of high molecular weight impurities with organic solvents (acetone and methanol), adsorption/desorption on the surface of activated carbon, extraction of the end product, crystallization, and ion exchange chromatography. The proteins and polysaccharides were removed from the CL by precipitation with acetone at 4 ^{0}C with subsequent adsorption/desorbtion of total ribonucleosides on activated carbon. The desorbed ribonucleosides were extracted from the reacted solid phase by eluting with EtOH-NH_3-solution at 60 ^{0}C; inosine – by extracting with 0.3 M ammonium–formate buffer (pH = 8.9) and subsequent crystallization in 80% (v/v) ethanol. The final purification consisted in column ion exchange chromatography on AG50WX 4 cation exchange resin

equilibrated with 0.3 M ammonium–formate buffer containing 0.045 M NH_4Cl with collection of fractions at R_f = 0.5. The curves *1–3* in Figure 5 shows UV-absorption spectra of inosine isolated from the CL at various stages of isolation procedure. The presence of major absorbance band I, corresponding to natural inosine (λ_{max} = 249 nm, ε_{249} = 7100 M^{-1} cm^{-1}), and the absence of secondary metabolites II and III in the analyzed sample (Figure 5, curve *3*), demonstrates the homogeneity of the isolated product and the efficiency of the isolation method.

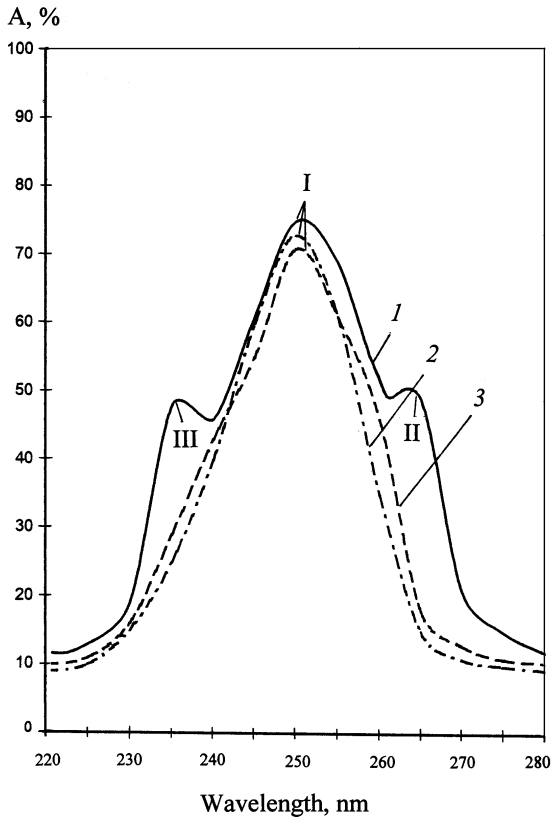

Figure 5. UV-absorption spectra of inosine (0.1 N HCl): (*1*) – initial LC after the growth of *B. subtilis* on HW medium; (*2*) – natural inosine, and (*3*) – inosine extracted from the LC. Natural inosine (*2*) was used as a control: (I) – inosine, (II, III) – secondary metabolites.

The level of deuterium enrichment of [^{2}H]inosine was determined by FAB mass spectrometry, the high sensitivity of which allows to detect 10^{-8} to 10^{-10} moles of a substance in a sample (Caprioli, 1990). The formation of a molecular ion peak for inosine in FAB mass spectrometry was accompanied by the migration of H^+. Biosynthetically ^{2}H-labeled inosine**,** which FAB mass-spectrum represented in Figure 6*b* regarding the control (natural protonated inosine, Figure 6*a*), represented a mixture of isotope-substituted molecules with different numbers of hydrogen atoms replaced by deuterium. Correspondingly, the molecular ion peak of inosine $[M+H]^+$, was polymorphically splintered into individual clusters with admixtures of molecules with statistical set of mass numbers *m/z* and different contributions to the total

level of deuterium enrichment of the molecule. It was calculated according to the most intensive molecular ion peak (the peak with the largest contribution to the level of deuterium enrichment) recorded by a mass spectrometer under the same experimental conditions. These conditions are satisfied the most intensive molecular ion peak $[M+H]^+$ at *m*/*z* 274 with 38% (instead of $[M+H]^+$ at *m*/*z* 269 with 42% under the control conditions; Figure 6*a*). That result corresponds to five deuterium atoms incorporated into the inosine molecule (Figure 6b). The molecular ion peak of inosine also contained less intensive peaks with admixtures of molecules containing four (*m*/*z* 273, 20%), five (*m*/*z* 274, 38%), six (*m*/*z* 275, 28%), and seven (*m*/*z* 276, 14%) deuterium atoms (Table 4).

Table 4. Values of peaks $[M+H]^+$ in the FAB mass spectra and levels of deuterium enrichment of inosine isolated from HW-medium.

Value of peak $[M+H]^+$	Contribution to the level of deuterium enrichment, mol.%	The number of deuterium atoms	Level of deuterium enrichment of molecules, % of the total number of hydrogen atoms*
273	20	4	20.0 ±0.60
274	38	5	62.5 ±1.80
275	28	6	72.5 ±1.96
276	14	7	87.5 ±2.98

Keys: *At calculation of the level of deuterium enrichment, the protons(deuterons) at the hydroxyl (OH^-) and imidazole protons at NH^+ heteroatoms were not taken into account because of keto–enol tautomerism in $H_2O/^2H_2O$.

Taking into account the contribution of the molecular ion peaks $[M]^+$, the total level of deuterium enrichment (TLDE) of the inosine molecule calculated using the below equation was 65.5% of the total number of hydrogen atoms in the carbon backbone of the molecule:

$$TLDE = \frac{[M]^+_{r1} \cdot C_2 + [M]^+_{r2} \cdot C_2 + ... + [M]^+_{rn} \cdot C_n}{\sum C_n}$$

where $[M]^+_r$ - the values of the molecular ion peaks of inosine.

C_n - the contribution of the molecular ion peaks to TLDE (mol %).

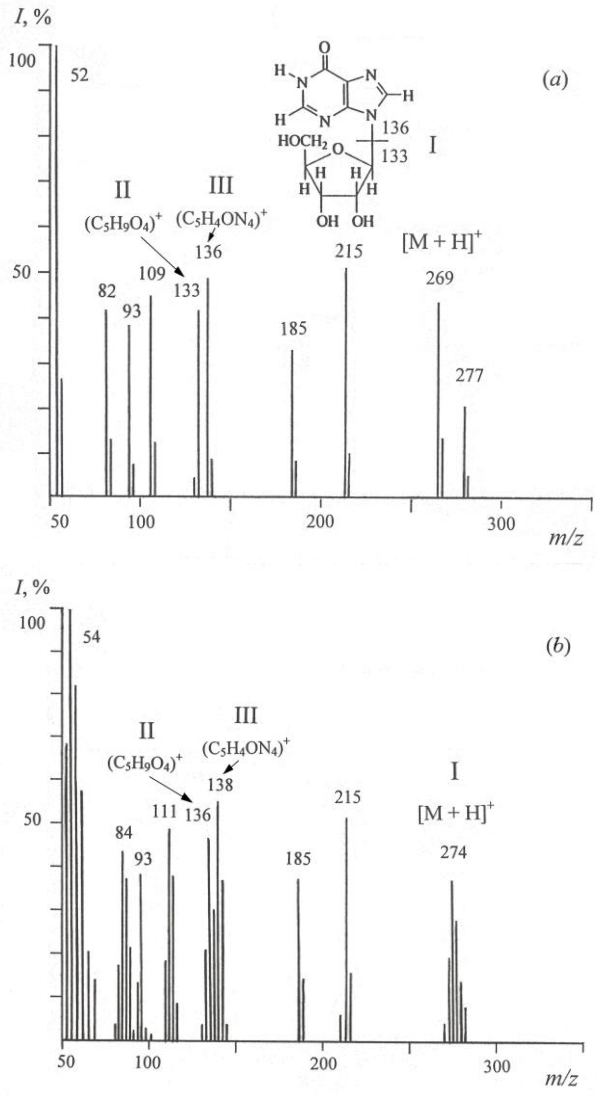

Figure 6. FAB mass spectra of inosine (glycerol as a matrix) under different experimental conditions: (*a*) – natural inosine; (*b*) – [^{2}H]inosine isolated from HW medium (scanning interval at *m*/*z* 50–350; major peaks with a relative intensity of 100% at *m*/*z* 52 and *m*/*z* 54; ionization conditions: cesium source; accelerating voltage, 5 kV; ion current, 0.6–0.8 mA; resolution, 7500 arbitrary units): *I* – relative intensity of peaks (%); (I) – inosine; (II) – ribose fragment; (III) – hypoxanthine fragment.

The fragmentation of the inosine molecule, shown in Figure 7, gives more precise information on the deuterium distribution in the molecule. The FAB fragmentation pathways of the inosine molecule (I) lead to formation of ribose $(C_5H_9O_4)^+$ fragment (II) at *m*/*z* 133 and hypoxanthine $(C_5H_4ON_4)^+$ fragment (III) at *m*/*z* 136 (their fragmentation is accompanied by the migration of H^+), which in turn, later disintegrated into several low-molecular-weight splinter fragments at *m*/*z* 109, 108, 82, 81, and 54 due to HCN and CO elimination from hypoxanthine (Figure 7). Consequently, the presence of two "heavy" fragments of ribose

II $(C_5H_9O_4)^+$ at *m*/*z* 136 (46%) (instead of *m*/*z* 133 (41%) in the control) and hypoxanthine III $(C_5H_4ON_4)^+$ at *m*/*z* 138 (55%) (instead of *m*/*z* 136 (48%) in the control), as well as the peaks of low molecular weight splinter fragments formed from FAB-decomposition of hypoxanthine fragment at *m*/*z* 111 (49%) (instead of *m*/*z* 109 (45%) in the control) and *m*/*z* 84 (43%) (instead of 82 (41%) in the control) suggests that three deuterium atoms are incorporated into the ribose residue, and two other deuterium atoms – into the hypoxanthine residue of the inosine molecule (Figure 7). Such selective character of the deuterium inclusion into the inosine molecule on specific locations of the molecule was confirmed by the presence of deuterium in the smaller fission fragments.

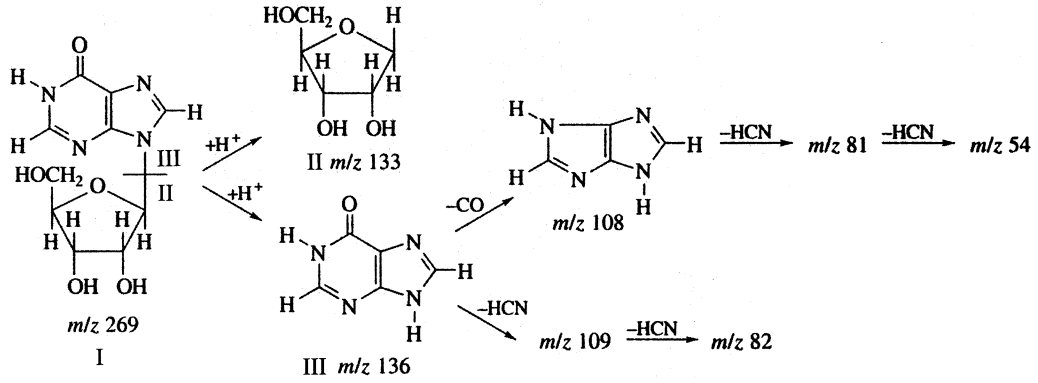

Figure 7. The fragmentation pathways of the inosine molecule leading to formation of smaller fragments by the FAB-method

When analyzing the level of deuterium enrichment of the inosine molecule we took into account the fact that the character of deuterium incorporation into the molecule is determined by the pathways of carbon assimilation. The carbon source was glucose as a main substrate and a mixture of deuterated amino acids from deuterated hydrolizate of methylotrophic bacterium *B. methylicum* as a source of deuterated substrated and amine nitrogen. Since the protons (deuterons) at positions of the ribose residue in the inosine molecule could have been originated from glucose, the character of deuterium inclusion into the ribose residue is mainly determined by hexose monophosphate (HMP) shunt, associated with the assimilation of glucose and other carbohydrates. HMP shunt is a complex of 12 reversible enzymatic reactions resulting in the oxidation of glucose to CO_2 to form reduced NADPH, and H^+, and the synthesis of phosphorylated sugars containing from 3 to 7 carbon atoms. Since glucose in our experiments was used in a protonated form, its contribution to the level of deuterium enrichment of the ribose residue was neglected. However, as the investigation of deuterium incorporation into the molecule by FAB method showed that deuterium was incorporated into the ribose residue of the inosine molecule owing to the preservation in this bacterium the minor pathways of *de novo* glucose biosynthesis in ^2H_2O-medium. Evidently the cell uses its own resources for intracellular biosynthesis of glucose from intracellular precursors. It should be noted that numerous isotopic ^1H–^2H exchange processes could also have led to specific incorporation of deuterium atoms at certain positions in the inosine molecule. Such accessible positions in the inosine molecule are hydroxyl

(OH^-)- and imidazole protons at NH^+ heteroatoms, which can be easily exchanged on deuterium in ^2H_2O *via* keto–enol tautomerism. Three non-exchangeable deuterium atoms in the ribose residue of inosine are synthesized *de novo* and could have been originated from HMP shunt reactions, while two other deuterium atoms at C2,C8-positions in the hypoxanthine residue could be synthesized *de novo* at the expense of [^{2}H]amino acids, primarily glutamine and glycine, that originated from deuterated hydrolysate of the methylotrophic bacterium *B. methylicum* obtained on 98 % of ^2H_2O medium. In particular, the glycoside proton at β-N_9-glycosidic bond could be replaced with deuterium *via* the reaction of CO_2 elimination at the stage of ribulose-5-monophosphate formation from 3-keto-6-phosphogluconic acid with subsequent proton (deuteron) attachment at the C1-position of ribulose-5-monophosphate. Two other protons at C2(C3) and C4 positions in ribose residue could be replaced with deuterium *via* further enzimatic isomerization of ribulose-5-monophosphate into ribose-5-monophosphate (Figure 8). In general, our studies confirmed this scheme (Ignatov & Mosin, 2013b). However, it should be noted that the level of deuterium enrichment of inosine molecule is determined by isotopic purity of ^2H_2O and deuterated substrates and, therefore, for the total administration of the deuterium label into the inosine molecule instead of protonated glucoce it must be used its deuterated analogue. Deuterated glucose may be isolated in gram-scale quntities from deuterated biomass of the methylotrophic bacterium *B. methylicum*.

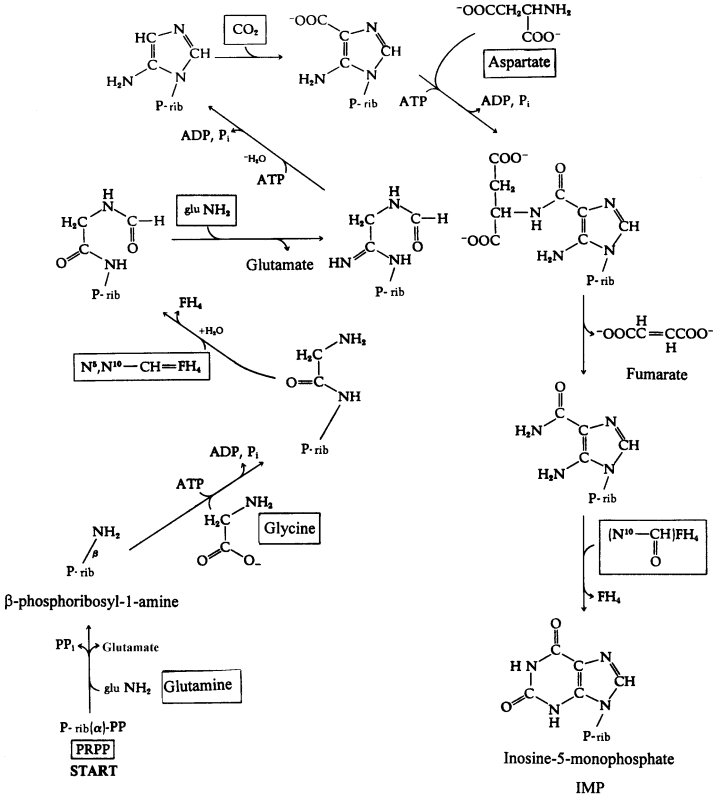

Figure 8. Scheme of biosynthesis of IMP by microbial cell (adapted from Bohinski, 1987)

3.3. Adaptation to deuterium the microalgae C. vulgaris

For adaptation of microalgae *C. vulgaris* was used Tamiya liquid mineral medium containing 25, 50, 75, and 98% (v/v) ^2H_2O (Mosin & Ignatov, 2012a). The levels of deuterium enrichment of carotenoids were In the case of *C. vulgaris* and *H. halobium* used fluorescent illumination, as both microorganisms grown in the presence of light. Individual colonies of cells of these microorganisms resistant to ^2H_2O, allocated by selection were grown on liquid growth media of the same composition with 99.9 atom% ^2H_2O for producing the deuterated biomass.

3.4. Adaptation to deuterium of photoorganotrophic halobacterium H. halobium

The cell membrane of extreme aerobic photo-organotrophic halobacterium *Halobacterium halobium* contains a chromoprotein trans-membrane protein - bacteriorhodopsin (BR) with the molecular weight ~26.5 kDa, determining the purple-red culour of halophilic bacteria. BR contains as chromophore group an equimolar mixture of 13-*cis*- and 13-*trans*-retinol C20 carotenoid, bound by aldemine bond schiff base (as in the visual animal pigments) with Lys-216 residue of the protein. In halobacteria BR functions as a light-driven transmembrane proton pump pumping a proton accros the membrane. Along with the BR the cell membrane of halobacteria contains a small amount of other related carotenoid pigments, the main of which bakterioruberin determining the stability of halobacteria to solar radiation (Oesterhelt & Stoeckenius, 1971; Oesterhelt, 1988).

The adaptation of photo-organotrophic halobacterium *Halobacterium halobium* was carried out via plating of initial cells to separate colonies on solid 2% (w/v) agarose HM2 media based on 99,9 atom% ^2H_2O and deuterated hydrolyzate biomass of *B. methylicum*, with the following subsequent selection of the colonies resistant to ^2H_2O. The growing of halobacteria was carried out under illumination by light fluorescent lamps LDS-40-2 (40 W) with monochromatic light with λ = 560 nm for 4–5 days at 35 ^{0}C as swoun in Figure 9. While growing of *H. halobium* on HM2 growth medium cells synthesized the purple carotenoid pigment, identified as a native BR on the the spectral ratio of protein and chromophore fragments in the molecule (D_{280}/D_{568} = 1.5:1.0). The growth of this bacterium on ^2H_2O medium was slightly inhibited as compared with the control on protonated growth medium that simplifies the optimization of conditions for the production of microbial biomass, which consists in the growing of the halobacterium on deuterated growth medium with 2% (w/v) of deuterated biomass hydrolyzate of *B. methylicum*, cell disintegration and lysis; isolation of purple membrane (PM) fraction; purification of PM from the low and high-molecular weight impurities, cellular RNA, carotenoids and phospholipids; solubilization of PM in 0.5% (w/v) solution of ionic detergent SDS–Na to form a microemulsion; fractionation of solubilized BR by MeOH; gel permeation chromatography (GPC) on Sephadex G-200 and electrophoresis in 12.5% (w/v) PAAG in 0.1% (w/v) SDS –Na (Mosin & Ignatov, 2014).

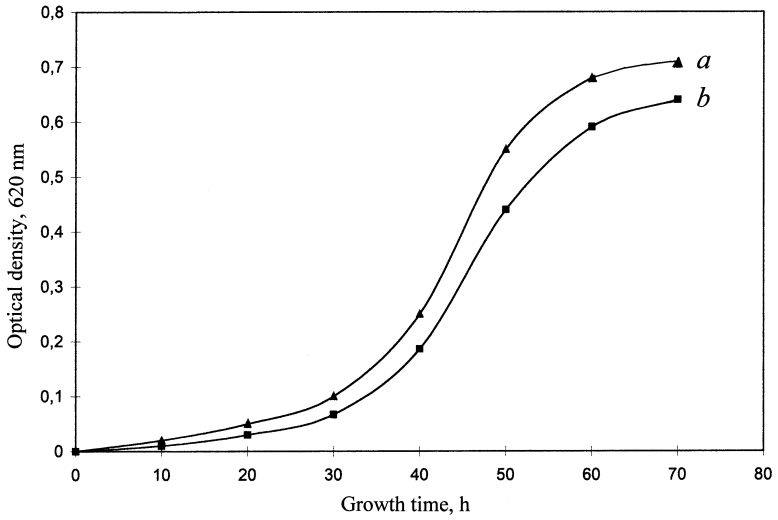

Figure 9. Growth dynamics of *H. halobium* under various experimental conditions: *a*) – HW2-medium; *b*) – peptone medium. Growing conditions: the incubation period: 4–5 days, temperature: 35 ^{0}C, illumination under monochrome light at λ = 560 nm

In an attempt to remove a large fraction of the carotenoids and phospholipids from the membrane by column GPC, PM fraction was washed by 50% (v/v) of EtOH before stabilization by SDS-Na. Removing of carotenoids, consisting in repeated treatment of PM with 50% (v/v) EtOH at 0 ^{0}C, was a routine but necessary step, in spite of the significant loss of the chromoprotein. It was used five treatments by 50% (v/v) EtOH to obtain the absorption spectrum of PM suspension purified from carotenoids (4) and (5) (degree of chromatographic purity of 80-85%), as shown in Figure 9 at various processing stages (*b*) and (*c*) relative to the native BR (a). Figure 10 shows a dark-adapted absorption maximum at λ = 548 nm. Formation of retinal-protein complex in the BR molecule leads to a bathochromic shift in the absorption spectrum of PM (Figure 10*c*) - the main bandwith (1) with the absorption maximum at λ = 568 nm caused by the light isomerization of the chromophore by the C13=C14 bond is determined by the presence of 13-*trans*-retinal residue in BR_{568}; additional low-intensity bandwith (2) at λ = 412 nm characterizes a minor impurity of a spectral form of meta-bacteriorhodopsin M_{412} (formed in the light) with deprotonated aldimine bond between 13-*trans*-retinal residue and protein; the total bandwith (3) with λ = 280 nm is determined by the absorption of aromatic amino acids in the polypeptide chain of the protein (for native BR D_{280}/D_{568} = 1.5:1.0). Upon light absorption, the maximum absorbance of PM shifts to λ = 556 nm with 6-8% increase in extinction. The 280/568 nm absorbance ratio of BR is directly related to the ratio of total protein (native BR) and is a convenient indicator for BR stability and integrity. Identical absorbance ratios are monitored using the conventional optics on a Beckman DU-6 spectrophotometer ("Beckman Coulter", USA) for detergent-solubilized BR or purified BR-solubilized in detergent.

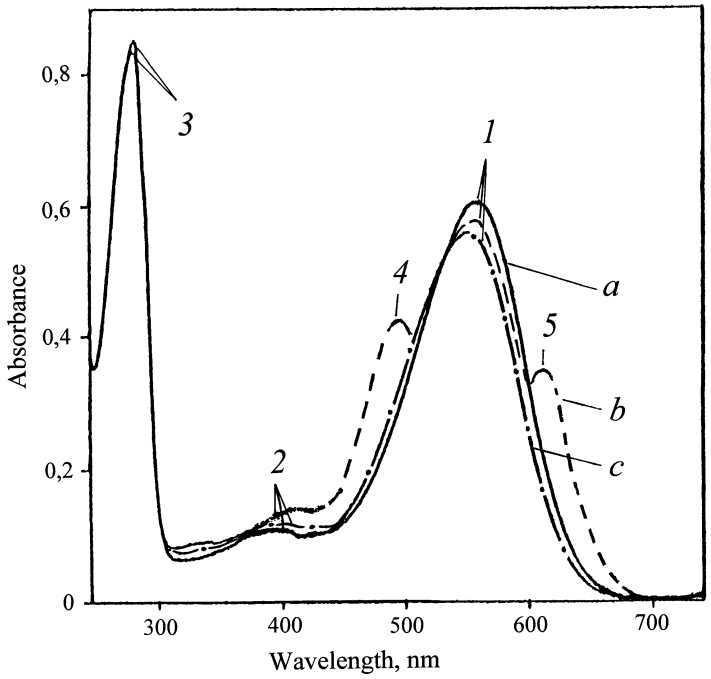

Figure 10. The absorption spectra of PM (50% (v/v) EtOH) at various stages of processing: (*a*) – natural BR; (*b*) – PM after intermediate treatment; (*c*) – PM purified from carotenoids. The bandwith (1) is the spectral form of BR_{568}, (2) – impurity of spectral form of meta-bacteriorhodopsin M_{412}, (3) – the total absorption bandwith of aromatic amino acids, (4) and (5) – extraneous carotenoids. As a control used the native BR.

The final stage of purification involved the crystallization of the solubilized in 0.5% (w/v) SDS-Na solution protein by MeOH and further separation of the protein from low-molecular-weight impurities by GPC. For this purpose the fractions containing BR were passed twice through a column with dextran Sephadex G-200 balanced with 0.09 M Tris buffer (pH = 8.35) containing 0.1% (w/v) SDS-Na and 2.5 mM EDTA.

The homogeneity of isolated BR satisfies to the requirements for reconstruction of native membranes, and was confirmed by electrophoresis in 12.5% (w/v) PAAG with 0.1% (w/v) SDS-Na and *in vitro* regeneration of AP with 13-*trans*-retinal. The degree of regeneration of PM was determined by the ratio: $D_{nat.280}{\cdot}D_{nat..568}/D_{reg..280}{\cdot}D_{reg.568}$ (D_{280} and D_{568} – the absorbance of a suspension of native and regenerated PM at $\lambda = 280$ and $\lambda = 568$ nm) was 65 mol.%. Output of crystalline protein makes up approximately 5 mg. The total level of deuterium enrichment of the BR molecule, calculated on deuterium enrichment levels of amino acids of the protein hydrolyzate was 95.7 atom% ^2H.

4. Discussion

Our studies indicated that the ability of adaptation to ^2H_2O for different taxonomic groups of

microorganisms is different, and stipulated by taxonomic affiliation, metabolic characteristics, pathways of assimilation of substrates, as well as by evolutionary niche occupied by the object. Thus, the lower the level of evolutionary organization of the organism, the easier it adapted to the presence of deuterium in growth media. Thus, most primitive in evolutionary terms (cell membrane structure, cell organization, resistance to environmental factors) of the studied objects are photo-organotrophic halobacteria related to archaebacteria, standing apart from both prokaryotic and eukaryotic microorganisms, exhibiting increased resistance to ^2H_2O and practically needed no adaptation to ^2H_2O, contrary to blue-green algae, which, being eukaryotes, are the more difficult adapted to ^2H_2O and, therefore, exhibit inhibition of growth at 70–75 % (v/v) D_2O.

The composition of growth media evidently also plays an important role in process of adaptation to ^2H_2O, because the reason of inhibition of cell growth and cell death can be changes of the parity ratio of synthesized metabolites in ^2H_2O-media: amino acids, proteins and carbohydrates. It is noted that adaptation to ^2H_2O occures easier on complex growth media than on the minimal growth media with full substrates at a gradual increasing of deuterium content in the growth media, as the sensitivity to ^2H_2O of different vital systems is different. As a rule, even highly deuterated growth media contain remaining protons ~0,2–10 atom.%. These remaining protons facilitate the restructuring to the changed conditions during the adaptation to ^2H_2O, presumably integrating into those sites, which are the most sensitive to the replacement of hydrogen by deuterium. The evidence has been obtained that cells evidently are able to regulate the $^2H/^1H$ ratios, while its changes trigger distinct molecular processes. One possibility to modify intracellular $^2H/^1H$ ratios is the activation of the H^+-transport system, which preferentially eliminates H^+, resulting in increased $^2H/^1H$ ratios within cells (Somlyai *et al*., 2012). Furthermore deuterium induces physiological, morphological and cytological alterations on the cell. There were marked the significant differences in the morphology of the protonated and deuterated cells of blue-green algae *C. vulgaris*. Cells grown on ^2H_2O-media were ~2–3 times larger in size and had thicker cell walls, than the control cells grown on a conventional protonated growth media with ordinary water, the distribution of DNA in them was non-uniform. In some cases on on the surface of cell membranes may be observed areas consisting of tightly packed pleats of a cytoplasmic membrane resembling mezosoms – intracytoplasmic bacterial membrane of vesicular structure and tubular form formed by the invasion of cytoplasmic membrane into the cytoplasm (Figure 11). It is assumed that mezosoms involved in the formation of cell walls, replication and segregation of DNA, nucleotides and other processes. There is also evidence that the majority number of mezosoms being absent in normal cells is formed by a chemical action of some external factors – low and high temperatures, fluctuation of pH and and other factors. Furthermore, deuterated cells of *C. vulgaris* were also characterized by a drastic change in cell form and direction of their division. The observed cell division cytodieresis did not end by the usual divergence of the daughter cells, but led to the formation of abnormal cells, as described by other authors (Eryomin *et al*., 1978). The observed morphological changes associated with the inhibition of growth of deuterated cells were stipulated by the cell restructuring during the process of adaptation to ^2H_2O. The fact that the deuterated cells are larger in size (apparent size was of ~2–4 times larger than the size of the protonated cells), apparently is a general biological phenomenn proved by growing a number of other adapted to ^2H_2O prokaryotic and eukaryotic cells (Mosin & Ignatov, 2012a; Mosin & Ignatov, 2012b; Mosin & Ignatov, 2014).

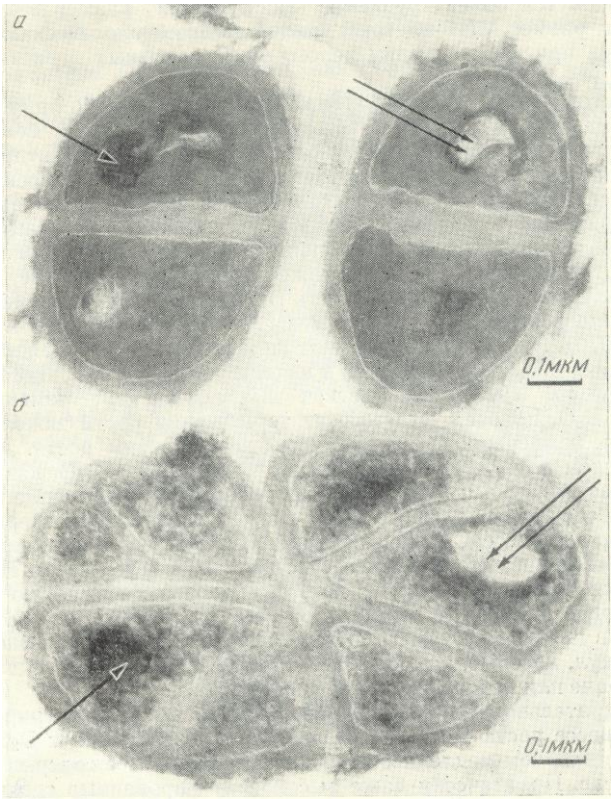

Figure 11. Electron micrographs of *Micrococcus lysodeikticus* cells obtained by SEM method: *a*) – protonated cells obtained on H_2O-medium; *b*) – deuterated cells obtained on ^2H_2O-medium. The arrows indicate the tightly-packed portions of the membranes

Our data generally confirm a stable notion that adaptation to ^2H_2O is a phenotypic phenomenon as the adapted cells eventually return back to the normal growth after some lag-period after their replacement back onto H_2O-medium. However, the effect of reversion of growth on $H_2O/^2H_2O$ media does not exclude an opportunity that a certain genotype determines the manifestation of the same phenotypic attribute in ^2H_2O-media with high deuterium content. At placing a cell onto ^2H_2O-media lacking protons, not only ^2H_2O is removed from a cell due to isotopic (^1H–^2H) exchange, but also there are occurred a rapid isotopic (^1H–^2H) exchange in hydroxyl (-OH), sulfohydryl (-SH) and amino (-NH_2) groups in all molecules of organic substances, including proteins, nucleic acids, carbohydrates and lipids. It is known, that in these conditions only covalent C–H bond is not exposed to isotopic (^1H–^2H) exchange and, thereof only molecules with bonds such as C–^2H can be synthesized de novo (Mosin et al., 1996b; Mosin & Ignatov, 2012a). Depending on the position of the deuterium atom in the molecule, there are distinguished primary and secondary isotopic effects mediated by intermolecular interactions. In this aspect, the most important for the structure of macromolecules are dynamic short-lived hydrogen (deuterium) bonds formed between the electron deficient $^1H(^2H)$ atoms and adjacent electronegative O, C, N, S- heteroatoms in the molecules, acting as acceptors of H-bond (Ignatov & Mosin, 2013c). The hydrogen bond, based on weak electrostatic

forces, donor-acceptor interactions with charge-transfer and intermolecular van der Waals forces, is of the vital importance in the chemistry of intermolecular interactions and maintaining the spatial structure of macromolecules in aqueous solutions (Ignatov & Mosin, 2013d). Another important property is defined by the three-dimensional structure of ^2H_2O molecule having the tendency to pull together hydrophobic groups of macromolecules to minimize their disruptive effect on the hydrogen (deuterium)-bonded network in ^2H_2O. This leads to stabilization of the structure of protein and nucleic acid macromolecules in the presence of ^2H_2O. That is why, the structure of macromolecules of proteins and nucleic acids in the presence of ^2H_2O is somehow stabilized (Cioni & Strambini, 2002).

Evidently the cell implements a special adaptive mechanisms promoting the functional reorganization of vital systems in ^2H_2O. Thus, for the normal synthesis and function in D2O of such vital compounds as nucleic acids and proteins contributes to the maintenance of their structure by forming hydrogen (deuterium) bonds in the molecules. The bonds formed by deuterium atoms are differed in strength and energy from similar bonds formed by hydrogen. Somewhat greater strength of ^2H–O bond compared to ^1H–O bond causes the differences in the kinetics of reactions in H_2O and ^2H_2O. Thus, according to the theory of a chemical bond the breaking up of covalent ^1H–C bonds can occur faster than C–^2H bonds, the mobility of $^2H_3O^+$ ion is lower on 28.5 % than H_3O^+ ion, and O^2H^- ion is lower on 39.8 % than OH^- ion, the constant of ionization of ^2H_2O is less than that of H_2O (Mosin et al., 1999b). These chemical-physical factors lead to slowing down in the rates of enzymatic reactions in D_2O (Cleland, 1976). However, there are also such reactions which rates in ^2H_2O are higher than in H_2O. In general these reactions are catalyzed by $^2H_3O^+$ or H_3O^+ ions or O^2H^- and OH^- ions. The substitution of ^1H with ^2H affects the stability and geometry of hydrogen bonds in an apparently rather complex way and may, through the changes in the hydrogen bond zero-point vibration energies, alter the conformational dynamics of hydrogen (deuterium)-bonded structures of DNA and proteins in ^2H_2O. It may cause disturbances in the DNA-synthesis during mitosis, leading to permanent changes on DNA structure and consequently on cell genotype (Lamprecht et al., 1989). Isotopic effects of deuterium, which would occur in macromolecules of even a small difference between hydrogen and deuterium, would certainly have the effect upon the structure. The sensitivity of enzyme function to the structure and the sensitivity of nucleic acid function (genetic and mitotic) would lead to a noticeable effect on the metabolic pathways and reproductive behaviour of an organism in the presence of ^2H_2O (Török et al., 2010). And next, the changes in dissociation constants of DNA and protein ionizable groups when transferring the macromolecule from H_2O into ^2H_2O may perturb the charge state of the DNA and protein molecules. All this can cause variations in nucleic acid synthesis, which can lead to structural changes and functional differences in the cell and its organelles. Hence, the structural and dynamic properties of the cell membrane, which depends on qualitative and quantitative composition of membrane's fatty acids, can also be modified in the presence of ^2H_2O. The cellular membrane is one of the most important organelles in the bacteria for metabolic regulation, combining apparatus of biosynthesis of polysaccharides, transformation of energy, supplying cells with nutrients and involvement in the biosynthesis of proteins, nucleic acids and fatty acids. Obviously, the cell membrane plays an important role in the adaptation to ^2H_2O. But it has been not clearly known what occurs with the membranes – how they react to the replacement of protium to deuterium and

how it concerns the survival of cells in $^{2}H_2O$-media devoid of protons.

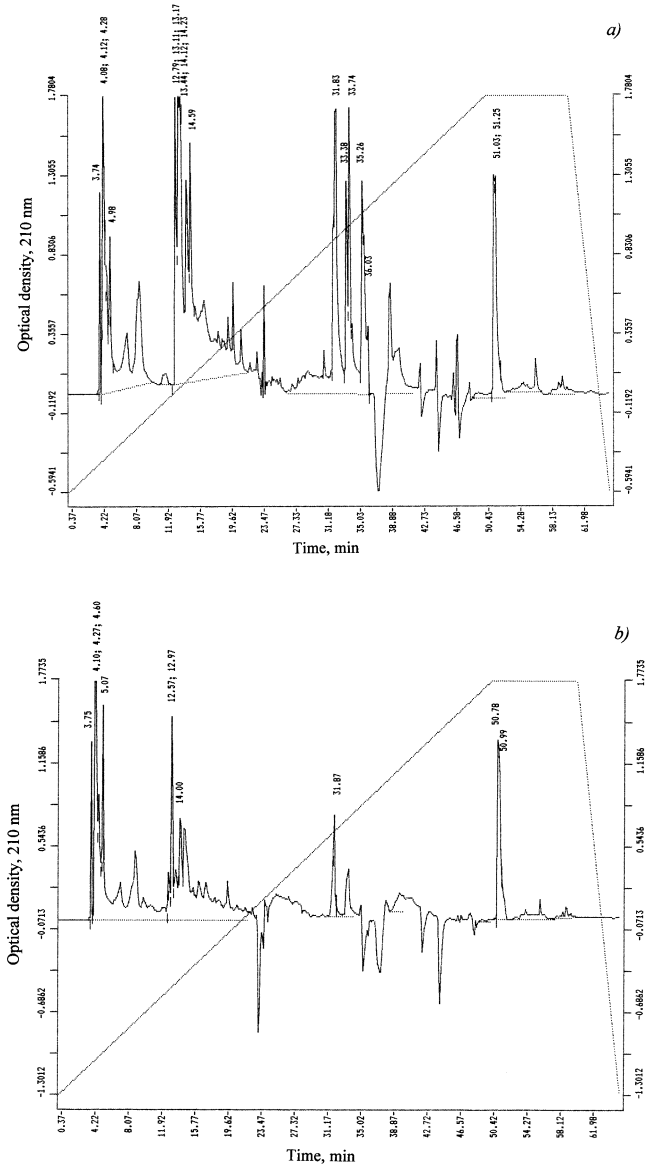

Figure 12. HPLC-chromatograms of fatty acids obtained from protonated (*a*) and deuterated (*b*) cells of *B. subtilis* on the maximally deuterated $^{2}H_2O$-medium: Beckman Gold System (Beckman, USA) chromatograph (4.6×250 mm); stationary phase: Ultrasphere ODS, 5 μm; mobile phase: linear gradient 5 mM KH_2PO_4–acetonitrile (shown in phantom), elution rate: 0.5 ml/min, detection at λ = 210 nm. The peaks with retention time 3.75 min (instead of 3.74 minutes in the control), 4.10; 4.27; 4.60 (instead of 4.08; 4.12; 4.28 in the control), 5.07 (instead of 4.98 in control) 12.57; 12.97 (instead of 12.79; 13.11; 13.17 in control) 14.00 (instead of 14.59 in the control), 31.87 (instead of 31.83 in the control); 33.38; 33.74; 33.26; 36.03; 50.78; 50.99 (instead of 51.03; 51.25 for control) correspond to individual intracellular fatty acids

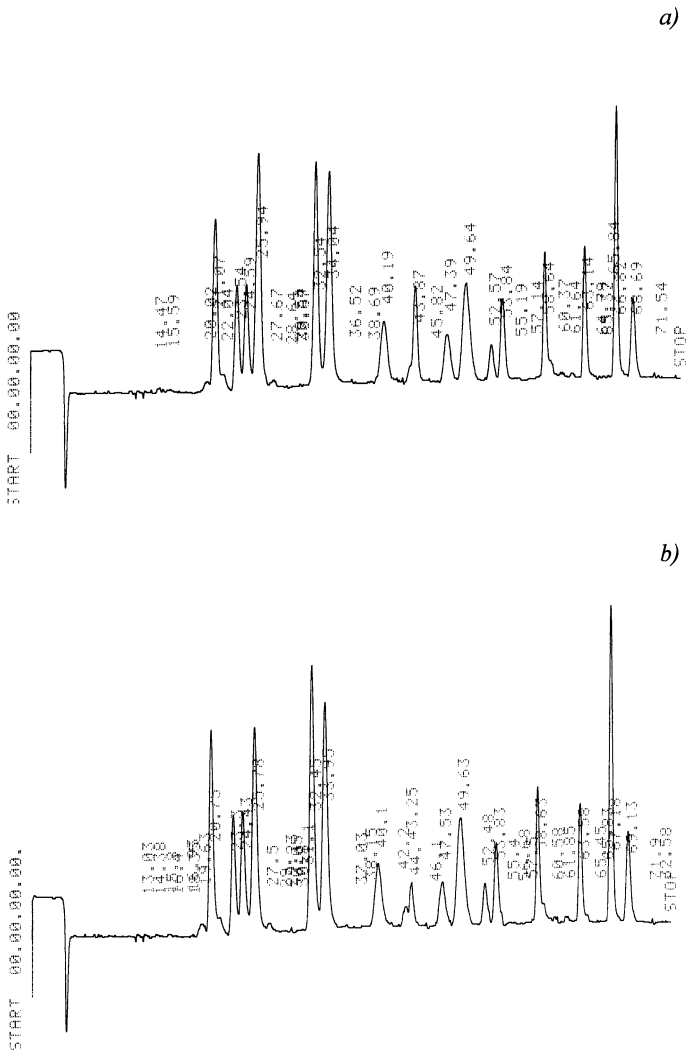

Figure 13. HPLC-chromatograms of amino acids obtained from hydrolizates of protonated (a) and deuterated (b) cells of *B. subtilis* on the maximally deuterated D_2O-medium: Biotronic LC-5001 (230×3.2 mm) column ("Eppendorf–Nethleler–Hinz", Germany); stationary phase: UR-30 sulfonated styrene resin ("Beckman–Spinco", USA); 25 μm; 50–60 atm; mobile phase: 0.2 N sodium–citrate buffer (pH = 2.5); the eluent input rate: 18.5 ml/h; the ninhydrin input rate: 9.25 ml/h; detection at λ = 570 and λ = 440 nm (for proline).

Comparative analysis of the fatty acid composition of deuterated cells of chemoheterotrophic bacteria *B. subtilis*, obtained on the maximum deuterated medium with 99.9 atom.% ^2H_2O (Figure 12b), carried out by HPLC method, revealed significant quantitative differences in the fatty acid composition compared to the control obtained in ordinary water (Figure 12a). Characteristically, in a deuterated sample fatty acids having

retention times at 33.38; 33.74; 33.26 and 36.03 min are not detected in HPLC-chromatogram (Fig. 12b). This result is apparently due to the fact that the cell membrane is one of the first cell organelles, sensitive to the effects of ^2H_2O, and thus compensates the changes in rheological properties of a membrane (viscosity, fluidity, structuredness) not only by quantitative but also by qualitative composition of membrane fatty acids. Similar situation was observed with the separation of other natural compounds (proteins, amino acids, carbohydrates) extracted from deutero-biomass obtained from maximally deuterated ^2H_2O-medium.

Table 5. Amino acid composition of the protein hydrolysates of *B. subtilis*, obtained on the maximum deuterated medium and levels of deuterium enrichment of molecules*

Amino acid	Yield, % (w/w) dry weight per 1 gram of biomass		Number of deuterium atoms incorporated into the carbon backbone of a molecule**	Level of deuterium enrichment of molecules, % of the total number of hydrogen atoms***
	Protonated sample (control)	The sample obtained in 99.9 atom.% ^2H_2O		
Glycine	8.03	9.69	2	90.0
Alanine	12.95	13.98	4	97.5
Valine	3.54	3.74	4	50.0
Leucine	8.62	7.33	5	50.0
Isoleucine	4.14	3.64	5	50.0
Phenylalanine	3.88	3.94	8	95.0
Tyrosine	1.56	1.83	7	92.8
Serine	4.18	4.90	3	86.6
Threonine	4.81	5.51	–	–
Methionine	4.94	2.25	–	–
Asparagine	7.88	9.59	2	66.6
Glutamic acid	11.68	10.38	4	70.0
Lysine	4.34	3.98	5	58.9
Arginine	4.63	5.28	–	–
Histidine	3.43	3.73	–	–

Notes:

* The data obtained by mass spectrometry for the methyl esters of N-5-(dimethylamino) naphthalene-1-sulfonyl chloride (dansyl) amino acid derivatives.

** While calculating the level of deuterium enrichment protons (deuterons) at the carboxyl (COOH-) and NH_2-groups of amino acid molecules are not taken into account because of their easy dissociation in $H_2O/^2H_2O$

*** A dash means absence of data.

Amino acid analysis of protein hydrolysates isolated from deuterated cells of *B. subtilis*, also revealed the differences in quantitative composition of amino acids synthesized in ^2H_2O-medium (Figure 13). Protein hydrolyzates contains fifteen identified amino acids (except proline, which was detected at λ = 440 nm) (Table 5). An indicator that determines a high efficiency of deuterium inclusion into amino acid molecules of protein hydrolyzates are high levels of deuterium enrichment of amino acid molecules, which are varied from 50 atom.% for leucine/isoleucine to 97.5 atom.% for alanine.

Qualitative and quantitative composition of the intracellular carbohydrates of *B. subtilis* obtained on maximally deuterated ^2H_2O-medium is shown in Table. 6 (the numbering is given to the sequence of their elution from the column) contained monosaccharides (glucose, fructose, rhamnose, arabinose), disaccharides (maltose, sucrose), and four other unidentified carbohydrates with retention time 3.08 min (15.63 %); 4.26 min (7.46 %); 7.23 min (11.72 %) and 9.14 min (7.95 %) (not shown) (Figure 14). Yield of glucose in deuterated sample makes up 21.4 % by dry weight, i.e. higher than for fructose (6.82 %), rhamnose (3.47 %), arabinose (3.69 %), and maltose (11.62 %). Their outputs are not significantly different from the control in H_2O except for sucrose in deuterated sample that was not detected (Table 6). The deuterium enrichment levels of carbohydrates were varied from 90.7 atom.% for arabinose to 80.6 atom.% for glucose.

Table 6. Qualitative and quantitative composition of intracellular carbohydrates of *B. subtilis* obtained on the maximally deuterated medium and levels of deuterium enrichment of molecules*

Carbohydrate	Content in the biomass, % of the dry weight of 1 g biomass		Level of deuterium enrichment, % of the total number of hydrogen atoms***
	Protonated sample (control)	The sample obtained in 99.9 atom.% ^2H_2O**	
Glucose	20.01	21.40	80.6
Fructose	6.12	6.82	85.5
Rhamnose	2.91	3.47	90.3
Arabinose	3.26	3.69	90.7
Maltose	15.30	11.62	–
Sucrose	8.62	ND	–

Notes:

* The data were obtained by IR-spectroscopy.

** ND – not detected

** A dash means the absence of data.

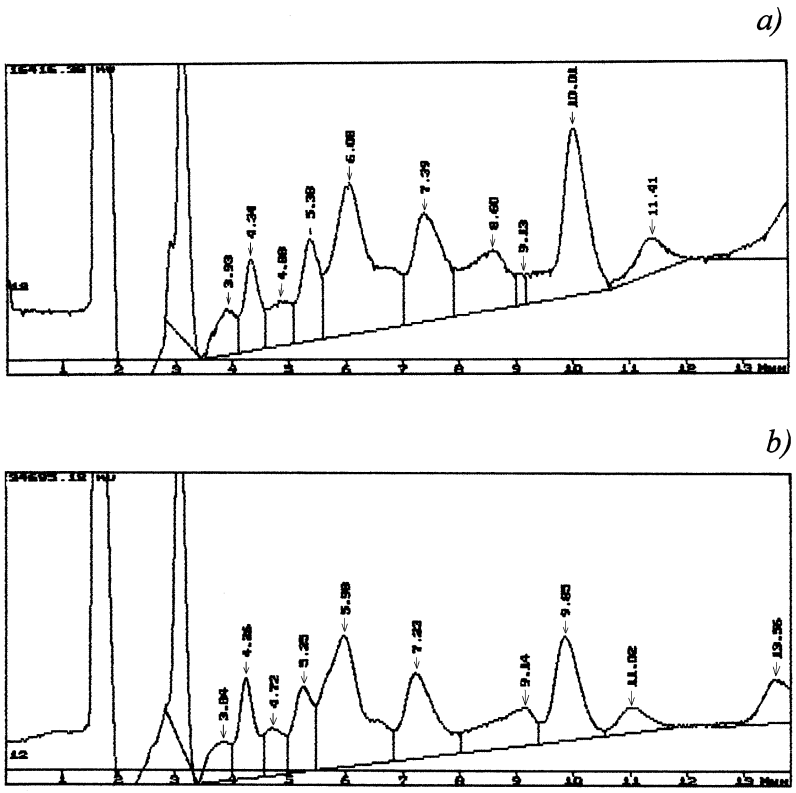

Figure 14. HPLC-chromatograms of intracellular carbohydrates obtained from protonated (a) and deuterated (b) cells of *B. subtilis* on the maximally deuterated ^2H_2O-medium: Knauer Smartline chromatograph (250×10 mm) ("Knauer", Germany); stationary phase: Ultrasorb CN; 10 μm; mobile phase: acetonitrile–water (75:25, % (w/w); the input rate: 0.6 ml/min

In conclusion it should be noted that comparative analysis of IR-spectra of H_2O solutions and its deuterated analogues (^2H_2O, H^2HO) is of considerable interest for biophysical studies, because at changing of the atomic mass of hydrogen by deuterium atoms in H_2O molecule their interaction will also change, although the electronic structure of the molecule and its ability to form H-bonds, however, remains the same. The local maximums in IR-spectra reflect vibrational-rotational transitions in the ground electronic state; the substitution with deuterium changes the vibrational-rotational transitions in H_2O molecule, that is why it appear other local maximums in IR-spectra. In the water vapor state, the vibrations involve combinations of symmetric stretch (v_1), asymmetric stretch (v_3) and bending (v_2) of the covalent bonds with absorption intensity (H_2O) $v_1;v_2;v_3$ = 2671; 1178.4; 2787.7 cm^{-1}. For liquid water absorption bands are observed in other regions of the IR-spectrum, the most intense of which are located at 2100, cm^{-1} and 710-645 cm^{-1}. For ^2H_2O molecule these ratio compiles 2723.7, 1403.5 and 3707.5 cm^{-1}, while for H^2HO molecule – 2671.6, 1178.4 and 2787.7 cm^{-1}. H^2HO (50 mole% H_2O + 50 mole% ^2H_2O; ~50 % H^2HO, ~25 % H_2O, ~25 % ^2H_2O) has local maxima in IR-spectra at 3415 cm^{-1}, 2495 cm^{-1} 1850 cm^{-1} and 1450 cm^{-1} assigned to OH^- -stretch, O^2H^- -stretch, as well as combination of bending and libration and H^2HO bending respectively.

In the IR-spectrum of liquid water absorbance band considerably broadened and shifted relative to the corresponding bands in the spectrum of water vapor. Their position depends on the temperature (Ignatov & Mosin, 2013*b*). The temperature dependence of individual spectral bands of liquid water is very complex (Zelsmann, 1995**).** Furthermore, the complexity of the IR-spectrum in the area of OH^- stretching vibration can be explained by the existence of different types of H_2O associations, manifestation of overtones and composite frequencies of OH^- groups in the hydrogen bonds, and the tunneling effect of the proton (for relay mechanism) (Yukhnevitch, 1973). Such complexity makes it difficult to interpret the spectrum and partly explains the discrepancy in the literature available on this subject.

In liquid water and ice the IR-spectra are far more complex than those ones of the vapor due to vibrational overtones and combinations with librations (restricted rotations, i.e. rocking motions). These librations are due to the restrictions imposed by hydrogen bonding (minor L_1 band at 395.5 cm^{-1}; major L_2 band at 686.3 cm^{-1}; for liquid water at 0 ^0C, the absorbance of L_1 increasing with increasing temperature, while L_2 absorbance decreases but broadens with reduced wave number with increasing temperature (Brubach et al., 2005). The IR spectra of liquid water usually contain three absorbance bands, which can be identified on absorption band of the stretching vibration of OH^- group; absorption band of the first overtone of the bending vibration of the molecule H^2HO and absorption band of stretching vibration of O^2H^- group (Max & Chapados, 2009). Hydroxyl group OH^- is able to absorb much infrared radiation in the infrared region of the IR-spectrum. Because of its polarity, these groups typically react with each other or with other polar groups to form intra-and intermolecular hydrogen bonds. The hydroxyl groups, which are not involved in formation of hydrogen bonds usually produce the narrow bands in IR spectrum, while the associated groups – broad intense absorbance bands at lower frequencies. The magnitude of the frequency shift is determined by the strength of the hydrogen bond. Complication of the IR spectrum in the area of OH^- stretching vibrations can be explained by the existence of different types of associations of H_2O molecules, a manifestation of overtones and combination frequencies of OH^- groups in hydrogen bonding, as well as the proton tunneling effect (on the relay mechanism).

Assignment of main absorbtion bands in the IR-spectrum of liquid water is given in the Table. 7. The IR spectrum of H_2O molecule was examined in detail from the microwave till the middle (4–17500 cm^{-1}) visible region and the ultraviolet region – from 200 nm^{-1} to ionization limit at 98 nm^{-1} (Walrafen, 1972). In the middle visible region at 4–7500 cm^{-1} are located rotational spectrum and the bands corresponding to the vibrational-rotational transitions in the ground electronic state. In the ultraviolet region (200 to 98 nm^{-1}) are located bands corresponding to transitions from the excited electronic states close to the ionization limit in the electronic ground state. The intermediate region of the IR-spectrum – from 570 nm to 200 nm corresponds to transitions to higher vibrational levels of the ground electronic state**.**

At the transition from H_2O monomers to H_2O dimer and H_3O trimer absorption maximum of valent stretching vibrations of the O-H bond is shifted toward lower frequencies (ν_3 = 3490 cm^{-1} and ν_1 = 3280 cm^{-1}) (Eisenberg & Kauzmann, 1969) and the bending frequency increased (ν_2 = 1644 cm^{-1}) because of hydrogen bonding. The increased strength of hydrogen bonding typically shifts the stretch vibration to lower frequencies (red-shift) with greatly increased intensity in the infrared due to the increased dipoles. In contrast,

for the deformation vibrations of the H-O-H, it is observed a shift towards higher frequencies. Absorption bands at 3546 and 3691 cm^{-1} were attributed to the stretching modes of the dimer [$(H_2O)_2$]. These frequencies are significantly lower than the valence modes of ν_1 and ν_3 vibrations of isolated H_2O molecules at 3657 and 3756 cm^{-1} respectively). The absorbtion band at 3250 cm^{-1} represents overtones of deformation vibrations. Among frequencies between 3250 and 3420 cm^{-1} is possible Fermi resonance (this resonance is a single substitution of intensity of one fluctuations by another fluctuation when they accidentally overlap each other). The absorption band at 1620 cm^{-1} is attributed to the deformation mode of the dimer. This frequency is slightly higher than the deformation mode of the isolated H_2O molecule (1596 cm^{-1}). A shift of the band of deformation vibration of water in the direction of high frequencies at the transition from a liquid to a solid atate is attributed by the appearance of additional force, preventing O-H bond bending. Deformation absorption band in IR-spectum of water has a frequency at 1645 cm^{-1} and a very weak temperature dependence. It changes little in the transition to the individual H_2O molecule at a frequency of 1595 cm^{-1}. This frequency is found to be sufficiently stable, while all other frequencies are greatly affected by temperature changes, the dissolution of the salts and phase transitions. It is believed that the persistence of deformation oscillations is stipulated by processes of intermolecular interactions, i.g. by the change in bond angle as a result of interaction of H_2O molecules with each other, as well as with cations and anions.

Table 7. The assignment of main frequencies in IR-spectra of liquid water H_2O and ^2H_2O

Main vibrations of liquid H_2O and ^2H_2O				
Vibration(s)	H_2O (t = 25 ^{0}C)		^2H_2O (t = 25 ^{0}C)	
	ν, cm^{-1}	E_0, M^{-1} cm^{-1}	ν, cm^{-1}	E_0, M^{-1} cm^{-1}
Spinning ν_1 + deformation ν_2	780-1645	21.65	1210	17.10
Composite $\nu_1 + \nu_2$	2150	3.46	1555	1.88
Valence symmetrical ν_1, valence asymmetrical ν_3, and overtone $2\nu_2$	3290-3450	100.65	2510	69.70

Thus the study of the characteristics of the IR spectrum of water allows to answer the question not only on the physical parameters of the molecule and the covalent bonds at isotopic substitution with deuterium, but also to make a certain conclusion on associative environment in water. The latter fact is important in the study of structural and functional properties of water assotiates and its isotopomers at the isotopic substitution with deuterium.

Conclusions

The experimental data demonstrated that the effects observed at the cellular growth on ^2H_2O-media possess a complex multifactor character stipulated by changes of morpholodical, cytological and physiological parameters – magnitude of the lag-period, time of cellular generation, outputs of biomass, a ratio of amino

acids, protein, carbohydrates and fatty acids synthesized in $^{2}H_2O$, and with an evolutionary level of organization of investigated object as well. The cell evidently implements the special adaptive mechanisms promoting functional reorganization of work of the vital systems in the presence of $^{2}H_2O$. Thus, the most sensitive to replacement of ^{1}H on ^{2}H are the apparatus of biosynthesis of macromolecules and a respiratory chain, i.e., those cellular systems using high mobility of protons and high speed of breaking up of hydrogen bonds. Last fact allows the consideration of adaptation to $^{2}H_2O$ as adaptation to the nonspecific factor affecting simultaneously the functional condition of several numbers of cellular systems: metabolism, ways of assimilation of carbon substrates, biosynthetic processes, and transport function, structure and functions of deuterated macromolecules. It seems to be reasonable to choose as biomodels in these studies microorganisms, as they are very well adapted to the environmental conditions and able to withstand high concentrations of $^{2}H_2O$ in growth media.

References:

Bohinski, R.C. (1987) *Modern Concepts in Biochemistry*, translated from English. Moscow: Mir Publishers Moscow, 544 [in Russian].

Brubach, J.B., Mermet, A., Filabozzi, A., Gerschel, A. & Roy, P. (2005) Signatures of the hydrogen bonding in the infrared bands of water. *J. Chem. Phys.*, **122**: 184509.

Caprioli R.M. (1990) *ContinuousFflow Fast Atom Bombardment mass Spectrometry*. N.Y.: Wiley: 125 .

Cioni, P. & Strambini, G.B. (2002) Effect of heavy water on protein flexibility. *Biophysical J.*, **82**(6): 3246–3253.

Cleland W.N. (1976) *Isotope effects on enzyme-catalyzed reactions*. W.N. Cleland, M.N. O'Leary & D.D. Northrop (eds.). Baltimore, London, Tokyo, University Park Press, 303.

Crespi H.L. (1989) Fully deuterated microorganisms: tools in magnetic resonance and neutron scattering. *Synthesis and applications of isotopically labeled compounds.* in: Proceedings of an International Symposium. T. Baillie & J.R. Jones (eds.) Amsterdam: Elsevier: 329–332.

Den'ko, E.I. (1970) Influence of heavy water (D_2O) on animal, plant and microorganism's cells. *Usp. Sovrem. Biol*., 70(4): 41–49.

Eisenberg, D. & Kauzmann, W. (1969) *The Structure and Properties of Water*. Oxford University Press, London.

Eryomin, V.A., Chekulayeva, L.N. & Kharatyan, F.F. (1978) Growth of *Micrococcus lysodeikticus* on a deuterated medium. *Microbiologia*, **14**: 629–636 [in Russian].

Ignatov I. & Mosin, O.V. (2013*a*) Possible processes for origin of life and living matter with modeling of physiological processes of bacterium *Bacillus subtilis* in heavy water as model system. *Journal of Natural Sciences Research*, **3**(9): 65-76.

Ignatov, I. (2005) *Energy Biomedicine*, Gea-Libris, Sofia, 1–88.

Ignatov, I. (2010) Which water is optimal for the origin (generation) of life? Euromedica, Hanover: 34-35.

Ignatov, I. (2011) Entropy and time in living matter, *Euromedica:* 74.

Ignatov, I. (2012) Origin of Life and Living Matter in Hot Mineral Water, Conference on the Physics, Chemistry and Biology of Water, Vermont Photonics, USA.

Ignatov, I., & Mosin, O.V. (2012) Isotopic Composition of Water and its Temperature in Modeling of Primordial Hydrosphere Experiments, VIII Intern. Conference Perspectives of the Development of Science and Technique, *Biochemistry and Biophysics*, **15**: 41–49.

Ignatov, I., Mosin, O. V. & Naneva, K. (2012) Water in the Human Body is Information Bearer about Longevity, *Euromedica*, Hanover: 110-111.

Ignatov I., Mosin O.V. (2013) Possible Processes for Origin of Life and Living Matter with Modeling of Physiological Processes of Bacterium *Bacillus Subtilis* in Heavy Water as Model System, *Journal of Natural Sciences Research*, **3** (9): 65-76.

Ignatov, I., Mosin, O. V. (2013) Modeling of Possible Processes for Origin of Life and Living Matter in Hot Mineral and Seawater with Deuterium, *Journal of Environment and Earth Science*, **3**(14): 103-118.

Ignatov, I., Mosin, O. V. (2013) Structural Mathematical Models Describing Water Clusters, *Journal of Mathematical Theory and Modeling*, **3** (11): 72-87.

Ignatov, I., Mosin, O. V. (2014) The Structure and Composition of Carbonaceous Fullerene Containing Mineral Shungite and Microporous Crystalline Aluminosilicate Mineral Zeolite. Mathematical Model of Interaction of Shungite and Zeolite with Water Molecules *Advances in Physics Theories and Applications*, **28**: 10-21.

Ignatov, I., Mosin, O.V., Velikov, B., Bauer, E. & Tyminski, G. (2014) Longevity Factors and Mountain Water as a Factor. Research in Mountain and Field Areas in Bulgaria, *Civil and Environmental Research*, **6** (4): 51-60.

Ignatov, I., Mosin, O. V., Niggli, H.&Drossinakis, Ch. (2014) Evaluating Possible Methods and Approaches for Registering of Electromagnetic Waves Emitted from the Human Body, Advances in Physics Theories and Applications, **30**: 15-33.

Ignatov, I., Mosin, O.V.&Drossinakis, Ch. (2014) Infrared Thermal Field Emitted from Human Body. Thermovision, *Journal of Medicine, Physiology, Biophysics,* **1:**1-12.

Ignatov, I., Mosin, O.V.&Velikov, B. (2014) Longevity Factors and Mountain Water of Bulgaria in Factorial Research of Longevity, *Journal of Medicine, Physiology, Biophysics*,**1**:13-33.

Ignatov, I.&Mosin,O.V. (2014) Visual Perception. Electromagnetic Conception for the Eyesight. Rhodopsin and Bacteriodopsin, Journal of Medicine, Physiology and Biophysics, 2:1-19.

Ignatov, I.&Mosin,O.V. (2014) The Structure and Composition of Shungite and Zeolite. Mathematical Model of Distribution of Hydrogen Bonds of Water Molecules in Solution of Shungite and Zeolite, Journal of Medicine, Physiology and Biophysics, 2: 20-36.

Ignatov, I., Mosin,O.V., Velikov, B., Bauer, E.&Tyminski, G. (2014) Research of Longevity Factors and Mountain Water as a Factor in Teteven Municipality, Bulgaria, Journal of Medicine, Physiology and Biophysics, 2: 37-52.

Ignatov, I.&Mosin,O.V. (2014) Modeling of Possible Processes for Origin of Life and Living Matter in Hot Mineral Water. Research of Physiological Processes of Bacterium Bacillus Subtilis in Hot Heavy Water, Journal of Medicine, Physiology and Biophysics, 2: 53-70.

Ignatov, I.&Mosin,O.V. (2014) Mathematical Models of Distribution of Water Molecules Regarding Energies of Hydrogen Bonds, Medicine, Physiology and Biophysics, 2: 71-94.

Katz, J.J. (1960) *The biology of heavy water*. Scientific American: 106-115.

Kushner, D.J., Baker, A. & Dunstall, T.G.. (1999) Pharmacological uses and perspectives of heavy water and deuterated compounds. *Can. J. Physiol. Pharmacol*., **77**(2): 79–88.

Laeng, R.H., Mini, R.L., Laissue, J.A. & Schindler R. (1991) Radioprotection of cultured cells by preincubation in medium containing deuterium oxide. *Int. J. Radiat. Biol*., **59**(1): 165–173.

Lamprecht, I. Schroeter, D. & Paweletz, N. (1989) Disorganization of mitosis in HeLa cells by deuterium oxide, *European journal of cell biology*, **50**(2): 360-369.

LeMaster, D.M. (1990) Uniform and selective deuteration in two-dimensional NMR studies of proteins. *Ann. Rev. Biophys. Chem*., **19**: 243–266.

Lis, G., Wassenaar, L.I. & Hendry, M.J. (2008) High-precision laser spectroscopy D/H and $^{18}O/^{16}O$ Measurements of microliter natural water samples. *Anal. Chem*., **80**(1): 287–293.

Lobishev, V.N. & Kalinichenko, L.P. (1978) *Isotopic effects of D_2O in biological systems*. Moscow, Nauka: 215 .

MacCarthy, P. (1985) Infrared spectroscopy of deuterated compounds: an undergraduate experiment. *J. Chem. Educ*., **62**(7): 633–638.

Maksimova, N.P., Dobrozhinetskaia, E.V. & Fomichev, Iu.K. (1990) Regulation of phenylalanine biosynthesis in the obligate methylotroph *Methylobacillus* M75. *Mol. Gen. Microbiol. Virusol.*, **10**: 28–30.

Max, J.J. & Chapados, C. (2009) Isotope effects in liquid water by infrared spectroscopy. III. H_2O and D_2O spectra from 6000 to 0 cm^{-1}. *J. Chem. Phys*., **131**: 184505.

Michel, F., Altermatt, H.J., Gebbers J.O. et al. (1988) Radioprotection by pretreatment with deuterated water: cytokinetic changes in the small intestine of the mouse. *Virchows. Arch. B. Cell. Pathol. Incl. Mol. Pathol*., **54**(4): 214–220.

Mosin, O.V. (1996a) Studying of methods of biotechnological preparation of proteins, amino acids and nucleosides, labeled with stable isotopes ^{2}H, ^{13}C and ^{15}N with high levels of isotopic enrichment: autoref. disser. thesis PhD: Moscow, M.V. Lomonosov State Academy of Fine Chemical Technology: 26 .

Mosin, O.V., Skladnev, D.A., Egorova, T.A. & Shvets, V.I. (1996b) Mass-spectrometric determination of levels of enrichment of ^{2}H and ^{13}C in molecules of amino acids of various bacterial objects. Bioorganic Chemistry, **22**(10–11): 856–869.

Mosin, O.V., Skladnev, D.A. & Shvets, V.I. (1996c) Methods for preparation of proteins and amino acids, labeled with stable isotopes ^{2}H, ^{13}C and ^{15}N. *Biotechnologia*, **3**: 12–32 [in Russian].

Mosin, O.V., Skladnev, D.A. & Shvets, V.I. (1998) Biosynthesis of ^{2}H-labeled phenylalanine by a new methylotrophic mutant *Brevibacterium methylicum*. *Bioscience, biotechnology, and biochemistry*, **62**(2): 225–229.

Mosin, O.V., Skladnev, D.A. & Shvets, V.I. (1999a) Incorporation of [2,3,4,5,6-^{2}H]phenylalanine, [3,5-^{2}H]tyrosine, and [2,4,5,6,7-^{2}H]tryptophan into bacteriorhodopsin molecule of *bacterium halobium*. *Applied Biochemistry and Microbiology*, **35**(1): 34–42.

Mosin, O.V., Skladnev, D.A. & Shvets, V.I. (1999b) Studying physiological adaptation of microorganisms

to heavy water. *Biotechnologya*, **8**: 16–23.

Mosin, O.V., Shvets, V.I., Skladnev, D.A. & Ignatov, I. (2012a) Studying of microbic synthesis of deuterium labeled L-phenylalanine by methylotrophic bacterium *Brevibacterium Methylicum* on media with different content of heavy water. *Russian Journal of Biopharmaceuticals*, **4**(1): 11–22.

Mosin, O.V. & Ignatov, I. (2012b) Isotope effects of deuterium in bacterial and microalgae cells at growth on heavy water (D_2O). *Voda: Himia i Ecologija*, 3, 83–94 [in Russian].

Mosin, O.V. & Ignatov, I. (2012c) Studying of isotopic effects of heavy water in biological systems on example of prokaryotic and eukaryotic cells. *Biomedicine, Moscow*, **1**(1–3): 31–50 [in Russian].

Mosin, O.V., Ignatov, I., Skladnev, D.A. & Shvets, V.I. (2013a) A strain of Gram-positive chemoheterotrophic bacterium *Basillus subtilis* – producer of [^{2}H]riboxine. *Drug development & registration*, **4**(5): 110–119 [in Russian].

Mosin, O.V., Shvets, V.I., Skladnev, D.A. & Ignatov, I. (2013b) Microbial synthesis of ^{2}H-labelled L-phenylalanine with different levels of isotopic enrichment by a facultative methylotrophic bacterium *Brevibacterium methylicum* with RuMP assimilation of Carbon. *Biochemistry (Moscow) Supplement Series B: Biomedical Chemistry*, **7**(3): 249–260.

Mosin, O.V. & Ignatov, I. (2013c) Studying the biosynthesis of ^{2}H-labeled inosine by a Gram-positive chemoheterotrofic bacterium *Bacillus subtilis* B-3157 on heavy water (^2H_2O) medium. *Chemical and Process Engineering Research*, **15**: 32–45.

Mosin, O.V., Shvez, V.I, Skladnev, D.A., & Ignatov, I. (2013d) Microbiological synthesis of [^{2}H]inosine with high degree of isotopic enrichment by Gram-positive chemoheterotrophic bacterium *Bacillus subtilis*. *Applied Biochem. Microbiol.*, **49**(3): 255–266.

Mosin, O.V. & Ignatov, I. (2013) Microbiological synthesis of ^{2}H-labeled phenylalanine, alanine, valine, and leucine/isoleucine with different degrees of deuterium enrichment by the Gram-positive facultative methylotrophic bacterium *Brevibacterium methylicum*. *International Journal of Biomedicine*, 3(2), 132–138.

Mosin, O.V., Ignatov, I., Skladnev, D.A. & Shvets, V.I. (2014) A strain of Gram-positive facultative methylotrophic bacterium *Brevibacterium methylicum* – producer of [^{2}H]phenylalanine. *Drug development & registration*, **1**(6): 58-67 [in Russian].

Mosin, O.V. & Ignatov, I (2014b) Biosynthesis of photochrome transmembrane protein bacteriorhodopsin of Halobacterium halobium labeled with deuterium at aromatic amino acids residues of 2,3,4,5,6-$^2H_5$]Phe, [3,5-$^2H_2$]Tyr and [2,4,5,6,7-$^2H_5$]Trp. *Chemistry and Materials Research*, **6**(3): 38-48.

Oesterhelt, D. & Stoeckenius, W. (1971) Rhodopsin - like protein from the purple membrane of *Halobacterium halobium*. *Nature*, **233**(89): 49–160.

Oesterhelt, D. (1988) The Structure and Mechanism of the Family of Retinal Proteins from Halophilic *Archaea Curr. Op. Struct. Biol.*, **8**: 489–500.

Sinyak, Y., Grigoriev, A., Gaydadimov, V., Gurieva, T., Levinskih, M. & Pokrovskii, B. (2003) Deuterium-free water in complex life-support systems of long-tern space missions. *Acta Astronautica*, **52**: 575.

Skladnev, D.A., Mosin, O.V., Egorova, T.A., Eremin, S.V. & Shvets, V.I. (1996) Methylotrophic bacteria

are sourses of isotopically labelled ^{2}H- and ^{13}C-amino acids. *Biotechnologija*, 5: 25–34 [in Russian].

Somlyai, G. (2001) The biological effect of deuterium-depleted water. A possible new tool in cancer therapy. *Anticancer Research Intern. J*., **21**(3): 23–33.

Somlyai, G. (2002) *The Biological Effect of Deuterium Depletion.* Budapest, Akademiai Klado, 130 .

Somlyai, G., Jancso, G., Jakli, G *et al*. (2012) Deuterium depletion from tissue culture to human clinical studies. In: *2nd International Congress on Deuterium Depletion*. Budapest, Hungary, 17–18 May, 2012.

Stom, D.I., Ponomareva, A.K., Vyatchina, O.F. (2006) Influense of water with varying content of deuterium on red Californian hybride (*Eusenia fetida Andrei Bouche*). *Bull. RAS*, **6**(52): 167–169 [in Russian].

Török, G., Csák, M., Pintér, A. *et al*. (2000) Effects of different deuterium concentrations of the media on the bacterial growth and mutagenesis. *Egészségtudomány/Health Science*, 44: 331-338.

Vertes A. (2003) *Physiological Effect of Heavy Water. Elements andIisotopes:Fformation, Transformation, Distribution*. Dordrecht: Kluwer Acad. Publ. 111–112.

Walrafen, G.E. (1972) Raman and infrared spectral investigations of water structure. In *Water a Comprehensive Treatise*, F. Franks, Ed., Vol. 1, Plenum Press, New York, 151–214.

Ykhnevitch, G.B. (1973) *Infrared spectroscopy of water*. Moscow, Nauka, 207 . [in Russian].

Zelsmann, H.R. (1995) Temperature dependence of the optical constants for liquid H_2O and D_2O in the far IR region. *J. Mol. Struct.*, **350**: 95–114.

The IISTE is a pioneer in the Open-Access hosting service and academic event management. The aim of the firm is Accelerating Global Knowledge Sharing.

More information about the firm can be found on the homepage:
http://www.iiste.org

CALL FOR JOURNAL PAPERS

There are more than 30 peer-reviewed academic journals hosted under the hosting platform.

Prospective authors of journals can find the submission instruction on the following page: http://www.iiste.org/journals/ All the journals articles are available online to the readers all over the world without financial, legal, or technical barriers other than those inseparable from gaining access to the internet itself. Paper version of the journals is also available upon request of readers and authors.

MORE RESOURCES

Book publication information: http://www.iiste.org/book/

IISTE Knowledge Sharing Partners

EBSCO, Index Copernicus, Ulrich's Periodicals Directory, JournalTOCS, PKP Open Archives Harvester, Bielefeld Academic Search Engine, Elektronische Zeitschriftenbibliothek EZB, Open J-Gate, OCLC WorldCat, Universe Digtial Library , NewJour, Google Scholar